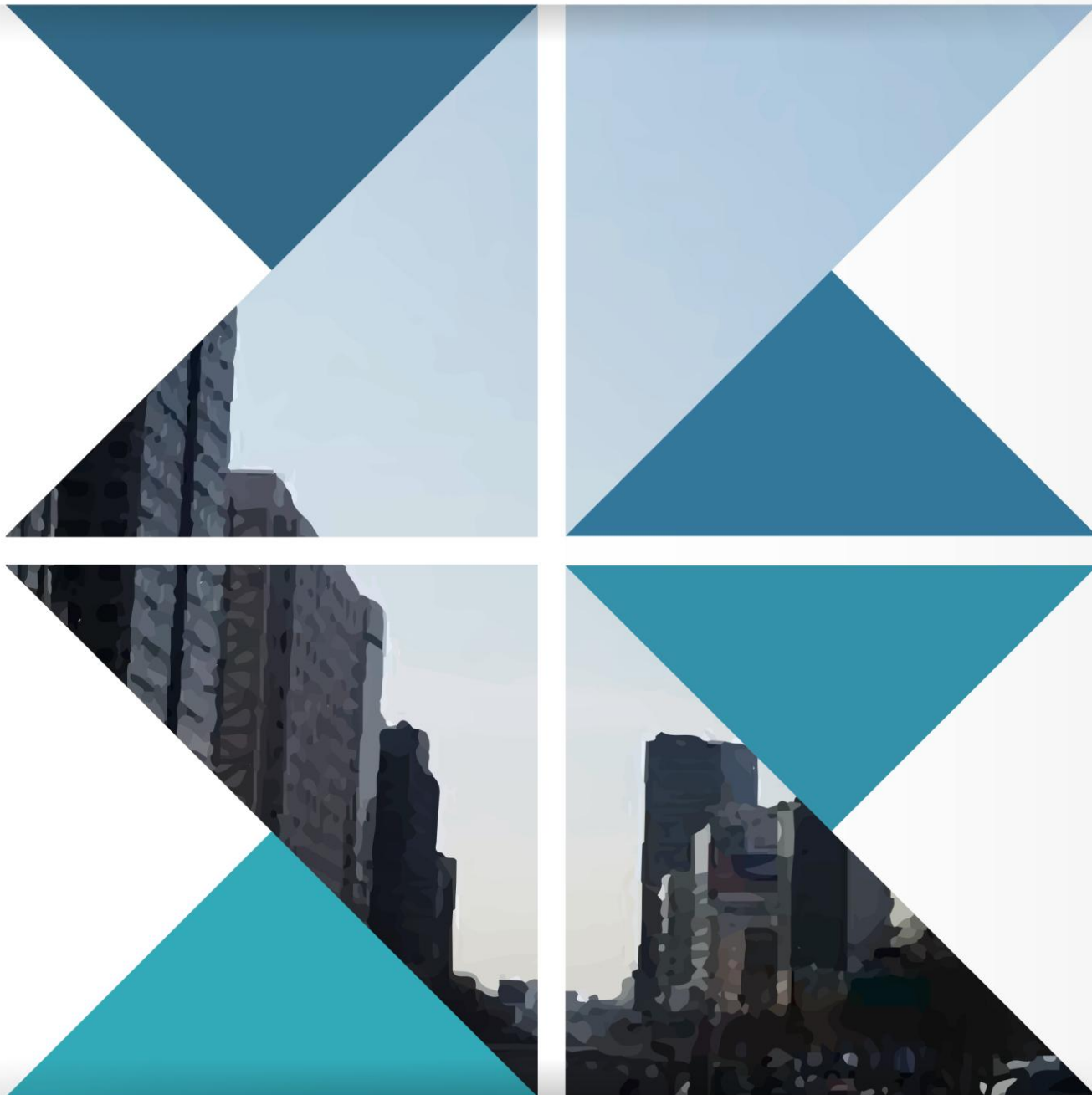


Non-Isothermal Kinetic Methods

Igor V. Arhangel'skii, Alexander V. Dunaev, Irina V. Makarenko, Nikolay. A. Tikhonov, Andrey V. Tarasov



Non-Isothermal Kinetic Methods

Max Planck Research Library for the History and Development of Knowledge

Series Editors

Jürgen Renn, Robert Schlögl, Bernard F. Schutz.

Edition Open Access Development Team

Lindy Divarci, Jörg Kantel, Matthias Schemmel and Kai Surendorf.

Scientific Board

Markus Antonietti, Ian Baldwin, Antonio Becchi, Fabio Bevilacqua, William G. Boltz, Jens Braarvik, Horst Bredekamp, Jed Z. Buchwald, Olivier Darrigol, Thomas Duve, Mike Edmunds, Yehuda Elkana, Fynn Ole Engler, Robert K. Englund, Mordechai Feingold, Rivka Feldhay, Gideon Freudenthal, Paolo Galluzzi, Kostas Gavroglu, Mark Geller, Domenico Giulini, Günther Görz, Gerd Graßhoff, James Hough, Manfred Laubichler, Glenn Most, Klaus Müllen, Pier Daniele Napolitani, Alessandro Nova, Hermann Parzinger, Dan Potts, Circe Silva da Silva, Ana Simões, Dieter Stein, Richard Stephenson, Mark Stitt, Noel M. Swerdlow, Liba Taub, Martin Vingron, Scott Walter, Norton Wise, Gerhard Wolf, Rüdiger Wolfrum, Gereon Wolters, Zhang Baichun.

Textbooks 1

**Edition Open Access
2013**

Non-Isothermal Kinetic Methods

Workbook and Laboratory Manual

I.V. Arkhangel'skii, A.V. Dunaev, I.V.
Makarenko, N.A. Tikhonov, S.S. Belyaev
and A.V. Tarasov

**Edition Open Access
2013**

Max Planck Research Library for the History and Development of Knowledge
Textbooks 1

Communicated by:
Robert Schlögl

Edited by:
Igor Arkhangel'skii

Editorial Coordination:
Beatrice Herrmann

Copyedited by:
Lindy Divarci

The current text was approved by Netzsch Gerätebau GmbH. and published with its kind permission.

ISBN 978-3-8442-4693-3

First published 2013 by Edition Open Access

<http://www.edition-open-access.de>

Printed in Germany by epubli, Oranienstraße 183, 10999 Berlin

<http://www.epubli.de>

Edition Open Access

<http://www.edition-open-access.de>

Published under Creative Commons by-nc-sa 3.0 Germany Licence

<http://creativecommons.org/licenses/by-nc-sa/3.0/de/>

The Deutsche Nationalbibliothek lists this publication in the Deutsche Nationalbibliografie; detailed bibliographic data are available in the Internet at <http://dnb.d-nb.de>.

The Max Planck Research Library for the History and Development of Knowledge comprises four subseries, *Studies*, *Proceedings*, *Sources* and *Textbooks*. They present research results and the relevant sources in a new format, combining the advantages of traditional publications and the digital medium. The volumes are available both as printed books and as online open access publications. They present original scientific work submitted under the scholarly responsibility of members of the Scientific Board and their academic peers.

The volumes of the four subseries and their electronic counterparts are directed at scholars and students of various disciplines, as well as at a broader public interested in how science shapes our world. They provide rapid access to knowledge at low cost. Moreover, by combining print with digital publication, the four series offer a new way of publishing research in flux and of studying historical topics or current issues in relation to primary materials that are otherwise not easily available.

The initiative is supported, for the time being, by research departments of three Max Planck Institutes, the MPI for the History of Science, the Fritz Haber Institute of the MPG, and the MPI for Gravitational Physics (Albert Einstein Institute). This is in line with the *Berlin Declaration on Open Access to Knowledge in the Sciences and Humanities*, launched by the Max Planck Society in 2003.

Each volume of the *Studies* series is dedicated to a key subject in the history and development of knowledge, bringing together perspectives from different fields and combining source-based empirical research with theoretically guided approaches. The studies are typically working group volumes presenting integrative approaches to problems ranging from the globalization of knowledge to the nature of spatial thinking.

Each volume of the *Proceedings* series presents the results of a scientific meeting on current issues and supports, at the same time, further cooperation on these issues by offering an electronic platform with further resources and the possibility for comments and interactions.

Each volume of the *Sources* series typically presents a primary source—relevant for the history and development of knowledge—in facsimile, transcription, or translation. The original sources are complemented by an introduction and by commentaries reflecting original scholarly work. The sources reproduced in this series may be rare books, manuscripts, documents or data that are not readily accessible in libraries and archives.

Each volume of the *Textbooks* series presents concise and synthetic information on a wide range of current research topics, both introductory and advanced. They use the new publication channel to offer students affordable access to high-level scientific and scholarly overviews. The textbooks are prepared and updated by experts in the relevant fields and supplemented by additional online materials.

On the basis of scholarly expertise the publication of the four series brings together traditional books produced by print-on-demand techniques with modern information technology. Based on and extending the functionalities of the existing open access repository European Cultural Heritage Online (ECHO), this initiative aims at a model for an unprecedented, Web-based scientific working environment integrating access to information with interactive features.

Contents

	Preface	1
	Introduction	3
1	Empirical Relationships and Specifics of Calculation Methods Used for Solving Non-Isothermal Kinetic Problems	5
2	Kinetic Experiment and Separation Methods	9
2.1	Heat Transfer Conditions	9
2.2	Mass Transfer Conditions	10
2.3	Nucleation	11
3	NETZSCH ThermoKinetics Software	15
3.1	Inverse Kinetic Problem	15
3.2	Direct Kinetic Problem	19
4	Kinetic Analysis Based on Thermogravimetry Data	23
4.1	Dehydration of Calcium Oxalate Monohydrate	23
4.2	Computational Procedure. Solution of the Inverse and Direct Ki- netic Problems. Quasi-One-Stage Process	24
4.3	Analysis of Computation Results	32
5	Kinetic Analysis Based on Differential Scanning Calorimetry Data	39
5.1	Computation Procedure. Solution of the Inverse and Direct Ki- netic Problems. Quasi-One-Stage Process	40
5.2	Analysis of Computation Results	45
5.3	Plotting the Conversion-Time Curves	49
6	Analysis of Multistage Processes	51
6.1	Peak Separation Software	51
6.2	Multiple Step Reaction Analysis as Exemplified by the Carboniza- tion of Oxidized PAN Fiber	53

Appendix	63
-----------------------	----

Preface

This application book is intended for senior students of natural science faculties of universities (faculties of chemistry, physics, geology, etc.) and technical institutes, who use methods of thermal analysis for kinetic studies in their research. The book can help researchers in studies of thermal decomposition, oxidation of various substances and materials, and other similar processes. It can be used in the laboratories of industrial enterprises applying methods of thermal analysis for quality control of raw materials and final products, and also by all users of the NETZSCH-Gerätebau GmbH equipment.

We would like to thank Dr. Gayana Kirakosyan (Institute of General and Inorganic Chemistry, Russian Academy of Sciences) for the translation into English and for useful remarks. We express our gratitude to Dr. Elena Moukhina (Netzsch-Gerätebau GmbH) for her explicit review and for the very helpful comments. We would like to thank in particular Dr. Malte Behrens and Prof. Robert Schlögl (Fritz-Haber Institute of the Max-Planck Society) for their support and assistance.

Introduction

The term “non-isothermal kinetics” appeared in the late 1950s as a result of the extensive development of thermoanalytical methods. At that time, the first commercial thermal analyzers appeared, providing sufficient precision and reproducibility of recorded data. It was also recognized that any thermoanalytical curve contains kinetic information on a process in a given temperature range. Numerous methods of estimating the Arrhenius parameters from the results of thermal analysis (TA) have been suggested [1]. However, later studies have shown that the experimental simplicity is in inverse proportion to the complexity of calculations for assessing the mechanisms of processes and determining their characteristics.

It is strongly recommended to become familiar with the work of Vyazovkin et al. [2]. This paper was developed by the Kinetics Committee of the *International Confederation for Thermal Analysis and Calorimetry* (ICTAC) as recommendations for reliable evaluation of kinetic parameters from the data obtained by means of thermal analysis methods.

Inasmuch as the TA experiment deals basically with solid samples, kinetic studies using thermoanalytical methods pertain to heterogeneous reactions. Kinetic analysis is based mainly on thermogravimetry (TG) and, to a lesser extent, on differential scanning calorimetry (DSC) data. The reasons for this are discussed below.

A formal kinetic analysis using TA data to describe heterogeneous reactions is based on certain empirical relationships, to which a physical meaning can be assigned, making allowance for certain a priori notions of the mechanism of reactions that occur in a system.

The reasoning behind the use of an empirical approach is as follows:

1. It is often rather difficult to suggest a physical and geometrical model that would correspond to the character of the process during the entire course of reaction in the temperature range under consideration. In addition, for poly-disperse systems in which parallel processes occur (as in macromolecular systems with molecules of different size), modeling is a rather challenging task, so that it is better to use a physical and mathematical description of the overall process.

2. For practical purposes, a detailed study of the reaction mechanism is of less importance than the optimization of the process by determining the effect of different experimental conditions on its rate.
3. The use of empirical relationships in kinetics makes it possible to easily obtain numerical characteristics. However, without an adequate analysis of results, it is impossible to give them a strict physical meaning. A typical example is the indiscriminate use of the concepts of homogeneous reaction kinetics to describe heterogeneous reactions.

This manual focuses on the use of the Netzsch software for formal kinetic description of heterogeneous reactions based on TA data. The program package comprises the following programs: the Thermokinetics program for solving inverse and direct kinetic problems, that is for estimating Arrhenius parameters, for finding the most statistically probable type of function to describe the process under consideration, and for performing predictive calculations; the Peak Separation program for decomposing multimodal curves into separate components; and the Thermal Simulation program considering scaling effects on the basis of Thermokinetics calculation results.

Chapter 1

Empirical Relationships and Specifics of Calculation Methods Used for Solving Non-Isothermal Kinetic Problems

The solving of the kinetic problem consists of several steps. At the first step the inverse kinetic problem is solved by evaluating of Arrhenius parameters. However, the solution requires a series of experiments with different heating rates and determination of optimal experimental conditions:

$$A_s \rightarrow B_s + C_g, \quad (1.1)$$

where A_s is the initial powdered solid reagent forming a flat layer, B_s is the solid reaction product located on the grains of the initial reagent, and C_g is the gaseous reaction product released into the environment. This process is referred to as quasi-one-stage, for reason that the reactions of the type of Equation 1.1 have at least three stages and comprise the chemical reaction stage, heat and mass transfer. However, depending on the experimental conditions, one of the stages can be limiting. In our case, we believe the chemical reaction to be the rate-limiting stage. Let us assume that the dependence of this process on time and temperature is a single-mode thermoanalytical curve.

For such a process, the change in the reaction rate as a function of temperature can be described as follows:

$$-\frac{d\alpha}{dt} = Ae^{\frac{-E}{RT}} f(\alpha), \quad (1.2)$$

where A and E are the Arrhenius parameters, T is the temperature, and $f(\alpha)$ is some function of the conversion of the reaction characterizing its mechanism. The conversion α , according to Equation 1.1, is defined as the fraction of the initial reagent A_s that has reacted by time t_i and changes from 0 to 1. It is worth noting that the conversion α can be calculated from both the TG and DSC data, as well as from differential thermogravimetry (DTG) data.

The so-called non-isothermal kinetic techniques are widely used owing to the apparent simplicity of processing experimental data according to the formal

kinetic model described by Equation 1.2. Equation 1.2 characterizes a single measurement curve.

As applied to experimental TA data, the kinetic model can be represented in the following form:

$$-\frac{d\alpha}{dT}_{T=T_i} = \frac{A}{\beta_i} \exp\left(-\frac{E}{RT}\right) \alpha_i^m (1 - \alpha_i)^n, \quad (1.3)$$

where $(1 - \alpha_i)$ is the experimentally measured degree of reaction incompleteness, T_i is the current temperature in kelvins (K), $\beta_i = dT/dt|_{T=T_i}$ is the instantaneous heating rate (in our experiment, $\beta_i = \beta = \text{constant}$), A is the preexponential factor, E is the activation energy, m and n are the kinetic equation parameter [1].

Equation 1.3 is easily linearized:

$$\ln\left(-\frac{d\alpha}{dT}_{T=T_i}\right) = \ln\left(\frac{A}{\beta_i}\right) - \frac{E}{RT_i} + m \cdot \ln \alpha_i + n \cdot \ln(1 - \alpha_i), \quad (1.4)$$

that is, it reduces to a linear least-squares problem.

The least-squares problem for Equation 1.4 reduces to solving the following set of equations:

$$C\vec{x} = \vec{b} \quad (1.5)$$

where C is the matrix of coefficients of Equation 1.4 ($C_{i1} = 1/\beta_i$, $C_{i2} = -1/T_i$, $C_{i3} = \ln \alpha_i$, $C_{i4} = \ln(1 - \alpha_i)$), and \vec{x} is the vector of the sought parameters. Since the experimental data are random numbers, they are determined with a certain error.

Solving the problem in Equation 1.5 involves certain difficulties.

The $1/T$ value changes insignificantly in the temperature range of reaction, therefore first and second column of matrix C are practically identical (up to a constant multiplier), and as a result matrix C is almost degenerate. Detailed description of this problem one can find in [3]. To minimize uncertainty one should provide several experiments with different heating rates and calculate kinetic parameters using all experimental data.

The above arguments suggest only that the calculation of Arrhenius parameters using a single thermoanalytical curve is incorrect. The Netzsch Termokinetics Software uses a different approach, when the Arrhenius parameters are estimated using model-free calculation methods according to a series of experiments at different heating rates (see below).

The inverse kinetic problem thus solved does not guarantee the adequate description of experimental data. To verify the adequacy of the solution, it is necessary to solve the direct problem, that is, to integrate Equation 1.3 and compare the calculated and experimental dependences in the entire range of heating rates. This procedure has been implemented in the NETZSCH Termokinetics, Peak Separation, and Thermal Simulation program packages with the help of NETZSCH. These programs and their applications are discussed in detail below.

Joint processing of experimental results obtained at different heating rates necessitates the constancy of the mechanism of a process, that is, the constancy of the type of $f(\alpha)$ function at different heating rates. Whether this condition is met can be verified by affine transformation of experimental curves, that is, by using reduced coordinates. To do this, one should select variables on the abscissa and ordinate so that each of them would change independently of the process under consideration. In addition, it is desirable that the relationship between the selected variables and experimental values be simple. These requirements are met by reduced coordinates. A reduced quantity is defined as the ratio of some variable experimental quantity to another experimental quantity of the same nature. As one of the variables, the conversion α is used, which is defined as the fraction of the initial amount of the reagent that has converted at a given moment of time. In heterogeneous kinetics, this variable is, as a rule, the conversion of the initial solid reagent.

If it is necessary to reflect the relationship between the conversion and time or temperature in the thermoanalytical experiment (at various heating rates), then the α is used as the ordinate and the reduced quantity equal to the ratio of the current time t or temperature T corresponding to this time to the time t_{α^*} it takes to achieve the desired conversion. For example, if the time or temperature required to achieve 50 or 90% conversion ($\alpha^* = 0.5$ or 0.9) is selected, the reduced quantities will be $t/t_{0.5}$ ($T/T_{0.5}$) or $t/t_{0.9}$ ($T/T_{0.9}$).

The above formalism pertains to the chemical stage of a heterogeneous process [4, 5]. However, it should be taken into account that in general case heterogeneous process may involve heat and mass transfer, that is, the process may be never strictly one-step. The multistage character of a process significantly complicates the solution of the kinetic problem. In this case, a set of at least three differential equations with partial derivatives should be solved, which often makes the problem unsolvable. At the same time, experimental conditions can be found under which one of the stages, most frequently, the chemical stage, would be the rate-limiting stage of the process. Such experimental conditions are found in a special kinetic experiment.

Chapter 2

Kinetic Experiment and Separation Methods

2.1 Heat Transfer Conditions

As is known, the thermoanalytical experiment is carried out under variable temperature conditions, most frequently at a constant heating rate. Thereby, a so-called quasi-stationary temperature gradient appears in the bottom-heated sample. The temperature at every point of a thermally inert cylindrical sample with radius R and height $H \leq 4R$ is described by the following equation:

$$T_i(r_i, t) = T_0 + \beta t - \frac{(\beta R^2 - r^2)}{4a} \left[1 + \frac{2\lambda}{hR} - \frac{r^2}{R^2} \right], \quad (2.1)$$

where $T_i(r_i, t)$ is the temperature at the i th point of the sample, T_0 is the starting temperature of the experiment, β is the temperature change rate $dT/dt = \text{constant}$, t is time, R is the radius of the cylindrical sample, r_i is the radius vector of a point of the sample, a is the thermal diffusivity, λ is the thermal conductivity, and h is the heat emission coefficient in the sample–holder system. Equation 2.1, which is an analytical representation of the solution to the heat transfer equation under certain assumptions, shows that a so-called quasi-stationary temperature regime is established in a sample, corresponding to a parabolic temperature field in the sample–holder system identical at any moment in time before the onset of thermal processes. Hence, the “conversion field” has the same shape, that is, each point of the sample is in its own state different from a neighboring one. Thus, different processes can occur at different points of the sample. In a chemical reaction accompanied by heat release or absorption (exo- and endothermic reactions), the temperature field can change significantly and temperature gradients can be as large as several tens of kelvins. To avoid this, conditions should be created under which the temperature gradients in the reacting system would not exceed the quasi-stationary gradient within the error of determination. This requirement is fulfilled under heat dilution conditions when the temperature field and heat exchange conditions are dictated by the thermophysical properties of the sample holder. This occurs in studying small amounts of a substance when the sample holder is made up of a metal with high heat conductance and its weight signif-

icantly exceeds the weight of the sample. Under these conditions, a so-called degenerate regime is realized, and heat exchange conditions have little effect on the kinetics of the process.

2.2 Mass Transfer Conditions

The mathematical description of mass transfer events accompanying heterogeneous processes is beyond the scope of this section. Rather, the aim is to show, at the qualitative level, how they can be experimentally affected. Let us consider the simplest heterogeneous process described by Equation 1.1.

In this process, several possible diffusion steps can be discerned. First, this is diffusion of gaseous products through the solid surface–environment interface. This mass transfer step can be controlled by purging the reaction volume with an inert gas. Figure 2.1 shows the results of studying the dehydration of $\text{CuSO}_4 \cdot 5\text{H}_2\text{O}$. The curve reflecting a three-stage process was obtained under dynamic environment conditions. The air flow rate was 40 mL/min. The curve indicates the loss of five water molecules; the water is removed stepwise, two molecules at a time in 40–180°C region and the fifth molecule is released at 210–270°C.

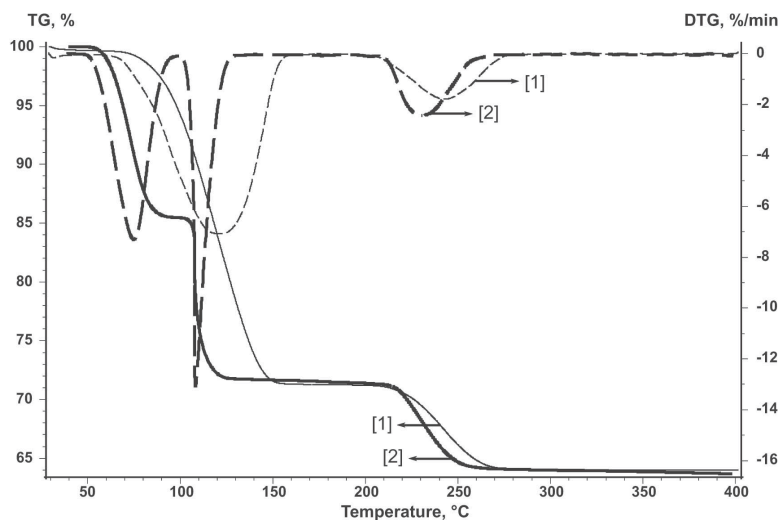


Figure 2.1: Dehydration of $\text{CuSO}_4 \cdot 5\text{H}_2\text{O}$ in an open crucible in a dry air flow (curve 2) and in a static atmosphere (curve 1).

The TG curve of a two-stage process pertains to the process in a static atmosphere. Figure 2.1 demonstrates that the process in a static atmosphere has another mechanism as compared with the process in an open crucible in the air flow. It is believed that diffusion hindrances arising in a static atmosphere are responsible for a significant effect of the back reaction. Since the $\text{CuSO}_4 \cdot 5\text{H}_2\text{O}$ dehydration is a reversible process, its kinetics changes noticeably. If changing the flow rate does not change the process rate, this step of mass transfer has no effect on the overall rate.

Second, the mass transfer in the porous medium of the initial reagent is worthy of consideration. The simplest way to verify the significance of this step is to carry out a series of experiments with a sample of different thickness at the same external surface area. If the change in the layer height has no effect on the process rate, the diffusion in the porous reagent can be approximately considered to have little effect on the process as a whole.

The step of mass transfer in the layer of the solid reaction product is the hardest to identify. A possible way to reveal diffusion limitations at this step is to determine how the composition changes in different parts of the solid reagent at various depths. However, this procedure is rather laborious and necessitates the use of appropriate analytical methods and a special sample preparation. To determine the role of diffusion limitations in the product layer, it is common practice to compare the propagation kinetics of the interface measured at different conversions. If diffusion hindrances exist, the Arrhenius parameters decrease with an increase in the product layer thickness. If the temperature coefficient of the reaction rate E/R (in general case it is better to use E/R instead of E , because E is measured in J/mol while for thermoanalytical data of any material or blend using of “mol” unit is meaningless) remains constant at different conversions, it can be stated that this type of diffusion is not a rate-limiting stage.

Thus, diffusion hindrances can manifest themselves at different steps of the process under consideration and can depend on both the design of equipment and the nature of substances involved in the process.

A conclusion that can be drawn from the above is that to mitigate a noticeable effect of transfer processes of experimental results, small amounts of the initial reagent (a few milligrams) with minimal porosity or lower heating rates should be used. In addition, it is important that the sample is placed on a rather large surface and that purge gases at a rather high flow rate are used.

2.3 Nucleation

If our experiment is carried out under conditions such that transfer phenomena have no effect on the shape of thermoanalytical curves, the reaction can be thought

of, to a first approximation, as a quasi-one-stage process representing the chemical transformations of reaction 1.1. However, the experimental results depend also on a change in the morphology of the initial reagent, i.e., on the formation of the reaction product, first of all, on the reagent surface. In this case, the conversion kinetics is dominated by the nucleation of the new phase and the subsequent growth of its nuclei. For heterogeneous processes, we are usually not aware of what atomic or molecular transformations lead to the nucleation of the product phase, so that the process is represented by a set of some formally geometric transformations. Non-isothermal kinetics is aimed at finding the forms of functions and their parameters describing these transformations.

Nucleation is related to the chemical stage of the process. However, because of the complexity and diversity of nucleation processes, we believe it is necessary to briefly dwell on this phenomenon, without going into theoretical descriptions of different steps of these processes. Consideration focuses on the manifestations of nucleation processes in the thermoanalytical experiment and on the proper design of the latter.

In the case of heterogeneous topochemical processes, the interface between the initial solid reagent and the solid reaction product is most frequently formed via nucleation processes. The reaction can simultaneously begin over the entire surface. In addition, nucleation can occur at separate sites of the surface, or by the branched chain mechanism, or another one. Possible mechanisms of these processes have been well documented (see, e.g., [1, 4, 5]). Here, we do not intend to go into details of all possible mechanisms; we will consider these phenomena in more detail when describing NETZSCH software.

For carrying out a kinetic experiment and obtaining reproducible results, it is necessary to standardize the surface of the initial reagent and create a definite amount of nuclei prior to the kinetic experiment. In the framework of thermoanalytical study, we can measure only the conversion (determination of the conversion or the overall reaction rate). Here, we do not consider the use of other physical methods for determining the number of nuclei on the reagent surface, for example, direct nucleus counting under the microscope. In thermal analysis, the most accessible and efficient method is natural nucleation under standard conditions. In this method, prior to the kinetic experiment, a noticeable amount of the initial reagent is heat treated up to a certain conversion. As a rule, the conversion amounts to several percent. The method is based on the fact that the last nucleation stages have little effect on the development of the reaction interface, since a large part of potential centers has already been activated. The sample thus standardized is used in all kinetic experiments, that is, at different heating rates.

Using the $\text{CuSO}_4 \cdot 5\text{H}_2\text{O}$ dehydration as an example, let us consider how the thermoanalytical curves change after natural nucleation under standard conditions as compared with the nonstandardized sample.

Figure 2.2 shows the TG and weight loss rate (DTG) curves for the initial untreated copper sulfate pentahydrate (curve 2) and for the sample subjected to natural nucleation under standard conditions (curve 1). To this end, the powder of the initial reagent was heated at $T = 70^\circ\text{C}$ until 10% H_2O was lost. As is seen, the shapes of the TG and DTG curves of the treated reagent differ from those of the initial reagent. Hence, the dehydration kinetics changes.

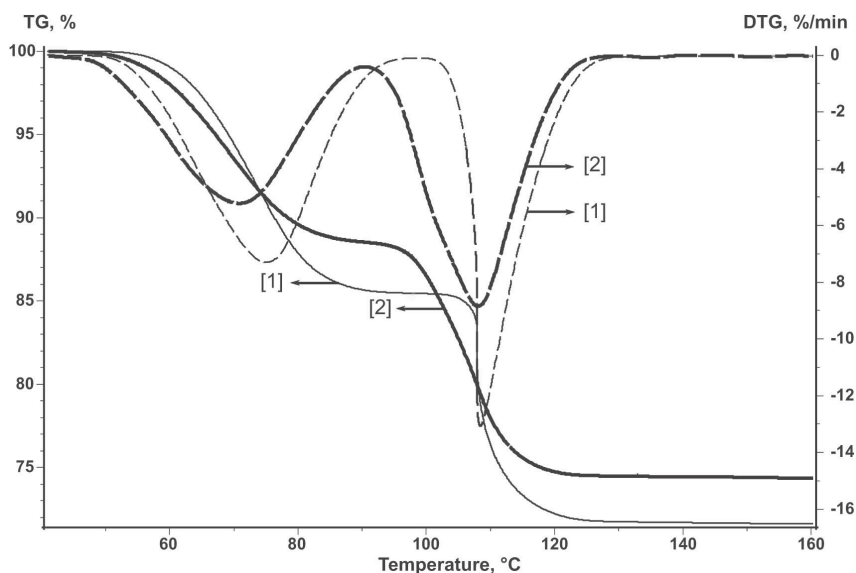


Figure 2.2: Dehydration of $\text{CuSO}_4 \cdot 5\text{H}_2\text{O}$ in an open crucible for the untreated sample (curve 2) and the standardized sample (curve 1).

Thus, using non-isothermal kinetics methods necessitates carrying out a special experiment involving a series of runs at various heating rates using the methods of separation of the rate-limiting stage, and small amounts of the solid reagent, purge gases, crucibles of appropriate size, and so forth.

Chapter 3

NETZSCH ThermoKinetics Software

The NETZSCH software suite intended for use in kinetic calculations from thermoanalytical data is based on the above principles. It naturally has specific features and computational procedure. Let us consider the software design philosophy and operational principles. In this workbook, Netzsch Proteus® 4.8.3 and Netzsch Thermokinetics® 3.0 versions are used to demonstrate main operating procedures. As Netzsch continuously improve software, we strongly recommend using actual versions of Proteus® and Thermokinetics®. New versions of software always include basic procedures presented in this workbook, as well as new useful functions.

3.1 Inverse Kinetic Problem

The inverse kinetic problem is solved with the use of model-free Friedman [6] methods and Ozawa–Flynn–Wall [7, 8] methods. The model-free methods (Friedman analysis, Ozawa–Flynn–Wall analysis, evaluation according to ASTM E698) are applied to non-isothermal kinetic analysis when experimental data is represented as the set of measurements at different heating rates. The model-free methods provide information on kinetic parameters, such as the activation energy and preexponential factor, without determining a concrete kinetic model. The Arrhenius parameters obtained by these methods are used as starting approximations in solving the direct kinetic problem. This solution makes it possible to find the type of function approximating the experimental data and to refine the Arrhenius parameters.

In thermal analysis, the concept of conversion is used. NETZSCH ThermoKinetics software operates with partial mass loss (for thermogravimetry), and partial area (for DSC, DTA and mass spectrometry) rather than with the common term conversion degree.

For integral measurements (thermogravimetry, dilatometry), the measured curve is converted to the plot of conversion α_i versus time t_i by Equation 3.1:

$$\alpha_i = \frac{m(t_s) - m(t_i)}{m(t_s) - m(t_f)}, \quad (3.1)$$

where (t_s) is the signal at the starting moment of time t_s , $m(t_i)$ is the signal at the i th moment of time t_i , and $m(t_f)$ is the signal at the final moment of time t_f .

For differential measurements (DSC, DTA, mass spectrometry), the conversion is calculated by Equation 3.2:

$$\alpha_i = \frac{\int_{t_s}^{t_i} [S(t) - B(t)] dt}{\int_{t_s}^{t_f} [S(t) - B(t)] dt}, \quad (3.2)$$

where $S(t)$ is the signal at the moment of time t and $B(t)$ is the baseline at the moment of time t .

3.1.1 Friedman Method

The Friedman method is a differential one, where the initial experimental parameter is the instantaneous rate $d\alpha_i/dt_i$.

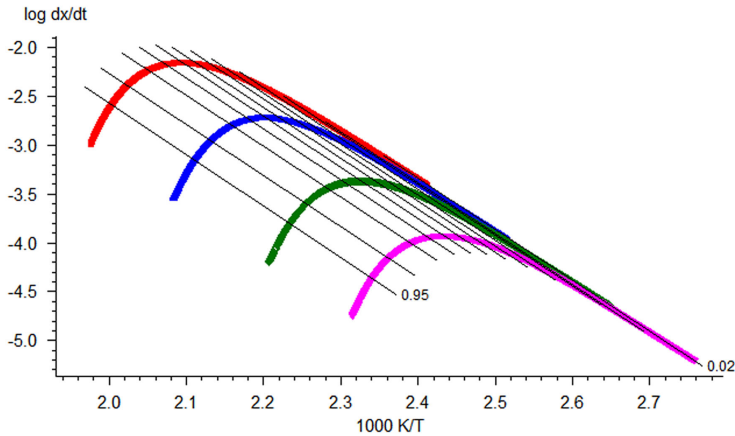


Figure 3.1: Friedman analysis for the simulated set of data for heating rates of 0.25, 1.0, 5.0, and 20.0 K/min (Reprinted with permission from [9] © NETZSCH-Gerätebau GmbH).

Providing several measurements at different heating rates one can plot a linear dependence of the logarithm of rate on inverse temperature for given α_i . As we notice above, Equation 1.4 can be easily linearized for any $f(\alpha)$ a linear dependence of the logarithm of rate on inverse temperature for given α_i . In the Friedman method, the slope $m = E/R$ of this line is found. Thus, the activation energy for each conversion rate can be calculated from the slope of the $\ln(d\alpha_i/dT)$ vs $1/T$ curve. The conversion rate on the left-hand side of the equation is found directly from the initial measured curve (e.g., thermogravimetric) by its differentiation with respect to time. This procedure is performed with the NETZSCH Proteus software used for processing the experimental data.

$$\ln\left(-\frac{d\alpha}{dT}\right)_{T=T_i} = \ln\left(\frac{A}{\beta_i}\right) - \frac{E}{RT_i} + \ln(f(\alpha_i)) \quad (3.3)$$

The second Arrhenius parameter, the logarithm of the preexponential factor, is also calculated from Equation 3.3.

Thus, the software allows the calculation of both Arrhenius parameters, the activation energy, and the logarithm of the preexponential factor. The calculation results are given in the tabulated form as the dependence of Arrhenius parameters on the conversion, as well as in the graphical form.

3.1.2 Ozawa–Flynn–Wall Method

The Ozawa method uses the integral dependence for solving Equation 1.3. Integration of the Arrhenius equation leads to Equation 3.4:

$$G(\alpha) = \int_0^1 \frac{d\alpha}{f(\alpha)} = \frac{A}{\beta} \int_{T_0}^T \exp\left(\frac{-E}{RT}\right) dt, \quad (3.4)$$

If T_0 is lower than the temperature at which the reaction occurs actively, the lower integration limit can be taken as zero, $T_0 = 0$, and after integration, Equation 3.5 takes the form of Equation 3.6:

$$\ln G(\alpha) = \ln\left(\frac{A \cdot E}{R}\right) - \ln \beta + \ln p(z) \quad (3.5)$$

$$p(z) = \frac{\exp(-z)}{z} - \int_{-\infty}^z \frac{\exp(-z)}{z} dz \text{ where } z = E/RT. \quad (3.6)$$

Analytical calculation of the integral in Equation 3.6 is impossible, therefore, it is determined as follows: Using the DOYLE approximation [7] ($\ln p(z) = -5.3305 + 1.052z$), we reduce Equation 3.5 to Equation 3.7:

$$\ln \beta = \ln\left(\frac{A \cdot E}{R}\right) - \ln G(\alpha) - 5.3305 + 1.052 \cdot \frac{E}{RT}. \quad (3.7)$$

It follows from Equation 3.7 that, for a series of measurements with different heating rates at the fixed conversion value $\alpha = \alpha_k$, the plot of the dependence

$$\ln \beta_i = f(1/T_{ik}) \quad (3.8)$$

is a straight line with the slope $m = -1.052 E/R$. T_{ik} is the temperature at which the conversion α_k is achieved at the heating rate β_i . It is evident that the slope of the linear dependence is directly proportional to the activation energy. If the activation energy has the same value at different α_k values, we can state with confidence that the reaction is one-stage. Otherwise, a change in the activation energy with an increase in the conversion is evidence that the process is multistep. The separation of the variables in Equation 1.3 is thus impossible.

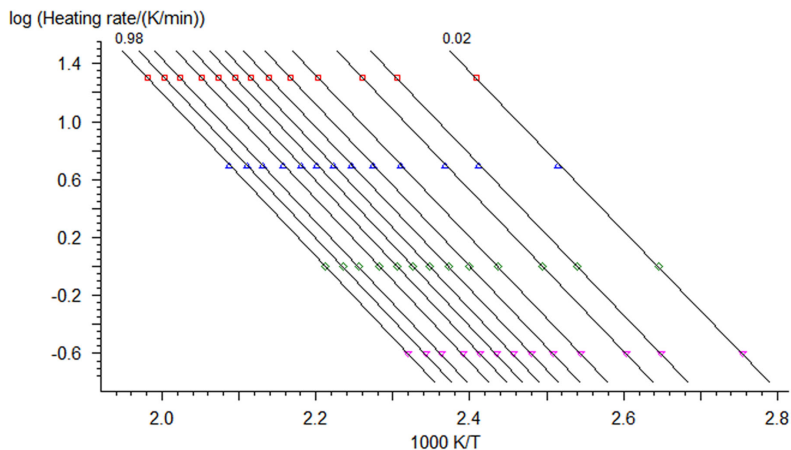


Figure 3.2: Dependences of the logarithm of rate on inverse temperature according to the Ozawa–Flynn–Wall procedure (Reprinted with permission from [9] © NETZSCH-Gerätebau GmbH).

If E , α_k , and z_i are known, $\ln A$ can be calculated by Equation 3.9:

$$\ln A = \ln G(\alpha) - \ln \frac{E}{R} + \ln \beta - \ln p(z), \quad (3.9)$$

Figure 3.2 shows the plots of instantaneous rate versus inverse temperature obtained by this method. The resulting Arrhenius parameters are then used as a zero approximation in solving the direct kinetic problem.

The presence of several extreme points on the experimental TA curves is unambiguous evidence of the multistep character of the process. In this case, the use of the NETZSCH Peak Separation program makes it possible to separate individual stages and to estimate the Arrhenius parameters for each stage. The Peak Separation program is discussed below.

3.2 Direct Kinetic Problem

The direct kinetic problem is solved by the linear least-squares method for one-stage reactions or by the nonlinear least-squares method for multistage processes. For one-stage reactions, it is necessary to choose the type of function that best approximates (from the statistical viewpoint) the experimental curves for all heating rates used. The NETZSCH Thermokinetics software includes a set of basic equations describing the macrokinetics of processes to be analyzed [10].

Each stage of a process can correspond to one (or several) of the equations listed in Table 3.1. The type of $f(\alpha)$ function depends on the nature of the process and is usually selected a priori. For the users convenience, the notation of parameters and variables in Table 3.1 is the same as in the Thermokinetics software. Here, the p parameter corresponds to the conversion, $p = \alpha$, and $e = 1 - \alpha$.

If the type of function corresponding to the process under consideration is unknown, the program performs calculations for the entire set of functions presented in Table 3.1. Then, on the basis of statistical criteria, the function is selected that best approximates the experimental data.

This approach is a formal statistical-geometric method and, to a first approximation, the type of function approximating the experimental curves for all heating rates has no physical meaning. Even for quasi-one-stage processes where the chemical conversion stage has been separated, the equations presented in Table 3.1 can be correlated with a change in the morphology of the initial reagent, but no unambiguous conclusions can be drawn about the types of chemical transformations responsible for the nucleation of the reaction product. It often occurs that several functions adequately describe the experiment according to statistical

Model abbreviation	$f(e,p)$	Reaction type
F1	e	First order
F2	e^2	Second order
F_n	e^n	n th order
D1	$0.5/1-e$	One-dimensional diffusion
D2	$-1/\ln(e)$	Two-dimensional diffusion
D3	$1.5e^{1/3}/(e^{-1/3}-1)$	Jander three-dimensional diffusion
D4	$1.5/(e^{-1/3}-1)$	Ginstling–Brounshtein three-dimensional diffusion
R2	$2e^{1/2}$	Reaction on the two-dimensional interface
R3	$3e^{2/3}$	Reaction on the three-dimensional interface
B1	ep	Autocatalysis according to the Prout–Tompkins equation
B_{na}	$e^n p^a$	n th order autocatalysis according to the Prout–Tompkins equation
C1-X	$e(1+K_{cat}X)$	First-order autocatalysis, X is the product in a complex model, often $X = p$
C_n -X	$e^n(1+K_{cat}X)$	n th autocatalysis
A2	$2e(-\ln(e))^{1/2}$	Two-dimensional nucleation (Avrami–Erofeev)
A3	$3e(-\ln(e))^{2/3}$	Three-dimensional nucleation (Avrami–Erofeev) f
A_n	$ne(-\ln(e))^{(n-1)/n}$	n -Dimensional nucleation (Avrami–Erofeev)

Table 3.1: Reaction types and corresponding type of function $f(\alpha)$ in Equation 1.2) [10].

criteria. The choice of the function is based on the search for the physical meaning of the resulting relation. In this context, some a priori ideas are used concerning the mechanisms of possible processes in the system under consideration. This can be literature data, results of other physicochemical studies, or general considerations based on the theories of heterogeneous processes. However, similar kinetic analysis provides a better insight into the effect of various external factors

on the change in the morphology of the initial reagent and on the course of the process as a whole. Let us consider in detail the procedure of kinetic analysis based on the thermoanalytical experimental data for the dehydration of calcium oxalate monohydrate ($\text{CaC}_2\text{O}_4 \cdot \text{H}_2\text{O}$).

Chapter 4

Kinetic Analysis Based on Thermogravimetry Data

4.1 Dehydration of Calcium Oxalate Monohydrate

Let us consider the dehydration as the reaction that occurs by the scheme $A_s \rightarrow B_s + C_g$, that is,

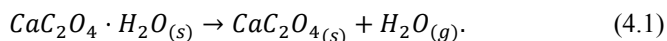


Figure 4.1 shows the TG curves of the dehydration of calcium oxalate monohydrate.

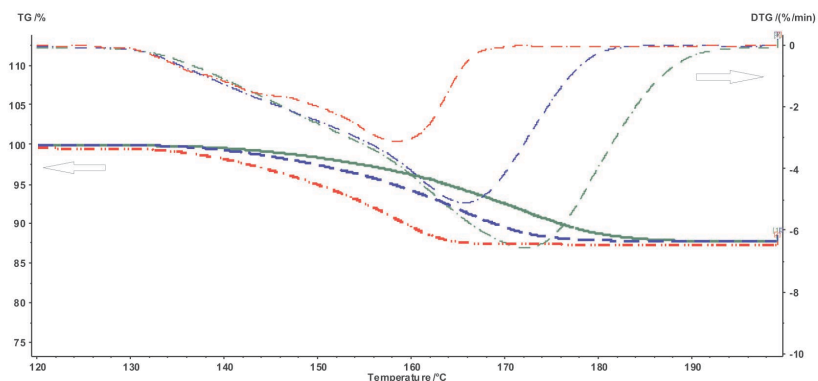


Figure 4.1: TG and DTG curves of the dehydration of calcium oxalate monohydrate at different heating rates.

The $CaC_2O_4 \cdot H_2O$ dehydration was studied on a Netzsch TG 209 F 3 Tarsus thermo-microbalance. The experiment was run at three heating rates: 5, 7.5, and 10 K/min. Three measurements were taken at each heating rate, other conditions being identical. Standard aluminum crucibles without lids were used as

holders. The process was carried out in a dry air flow at a rate of 200 mL/min. The initial reagent was freshly precipitated calcium oxalate with a particle size of 15–20 μm . Weighed portions of the reagent were 5–6 mg for each heating rate.

4.2 Computational Procedure. Solution of the Inverse and Direct Kinetic Problems. Quasi-One-Stage Process

As follows from Figure 4.1, the dehydration in the given temperature range can be considered a quasi-one-stage reaction at all heating rates used. The experimental data obtained on NETZSCH equipment are processed with the NETZSCH Proteus software.

For further work with the experimental data using the NETZSCH Thermokinetics software, it is necessary to export data from the Proteus program in the tabulated form (measured signal as a function of temperature or time) as an ASCII file. To do this, the user must select the desired curve and click the Extras \rightarrow Export data button in the Proteus toolbar. The user must enter the lower and upper limits of the data range to be exported. To correctly specify the limits, the derivative of the selected curve is used. The left- and right-hand limits are chosen in the ranges where the derivative becomes zero (Figure 4.2).

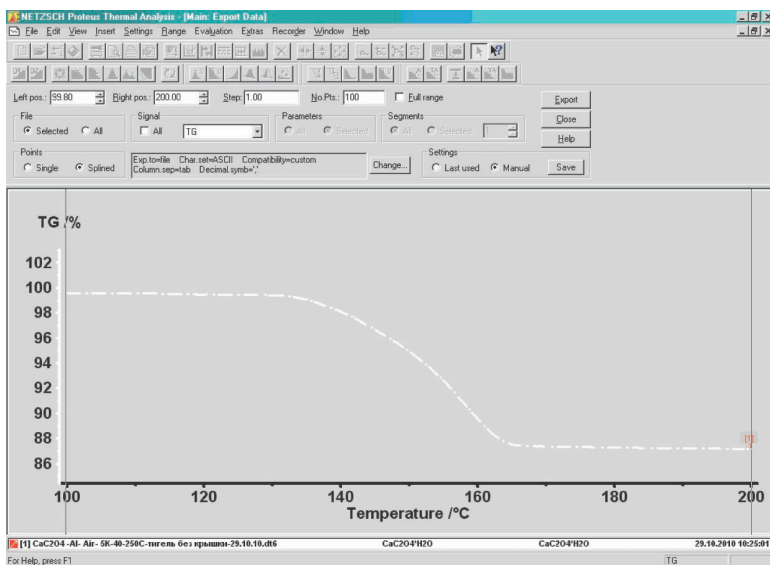


Figure 4.2: Selection of the number of points while exporting data.

Remember that the derivative of the selected curve can be obtained by clicking the corresponding icon in the NETZSCH Proteus program window.

An important step for further calculations is to select the number of points on the TG curve used for subsequent processing. This can be done in two ways. While exporting the data from the NETZSCH Proteus software, the user enters either the number of points of the curve to be exported (input window No.Pts., Figure 4.2) or the temperature increment between neighboring points (window Steps, Figure 4.2) from which the program calculates the number of points. In our case, from the parallel measurements performed under identical conditions, the root-mean-square deviation of the temperature for the rate curve minimum (DTG) was calculated to be $S \cong 1\text{K}$. For the selected temperature range, 100 points for each curve are used. It is worth noting that the use of a smaller increment is physically unreasonable since the S value reflects the properties of the system in question, but is not the temperature measurement accuracy provided by an instrument, which is an order of lower magnitude. In this case, specific features of the process should be taken into account.

If necessary, the experimental curves can be smoothed before exporting data, using the NETZSCH Proteus Analysis program (Figures 4.3, 4.4). The smooth level (Figure 4.4) is considered sufficient when the DTG curve has no spikes.

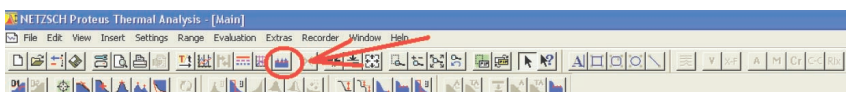


Figure 4.3: Curve smoothing.

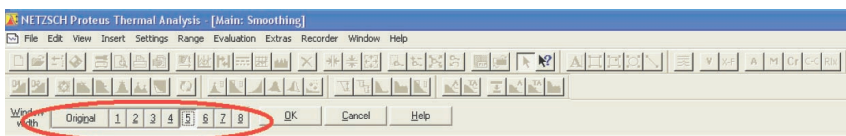


Figure 4.4: Selection of the curve smooth level.

After all data has been imported as ASCII files, they can be used for kinetic analysis with the NETZSCH Thermokinetics software. To do this, a new project is created (Figure 4.5). In the initialization dialog box, the project name, the sample, the number of measured curves (scans), and the type of measurement (TG, DSC, etc.) are entered.

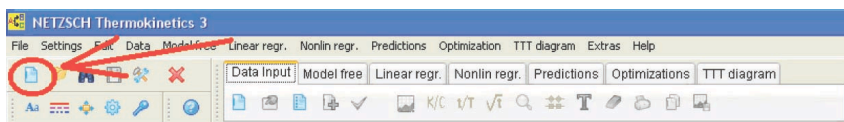


Figure 4.5: Creation of a new project in the NETZSCH Thermokinetics software.

Project Initialization

Project name:

Material:

No of Scans[1..16]:

Type of measurement:

Direction of exotherm:

Parameters of Diff. contr.:

Type of math. weight:

Correction parameters:

Tested models:

#	Code	Type 1	Type 2	Type 3	Type 4	Type 5
1						
2						
3						

Remarks:

Buttons: OK, Cancel, Change Corr Par, Negative E, Clear Remarks

Figure 4.6: Initiation of a new project in the NETZSCH Thermokinetics software.

The user imports then the data into the program. To do this, the type of loaded data should be specified (Figure 4.7). In the dialog box (Figure 4.8), the type of measurement is specified. In the case of thermogravimetry, GTA TG is selected.

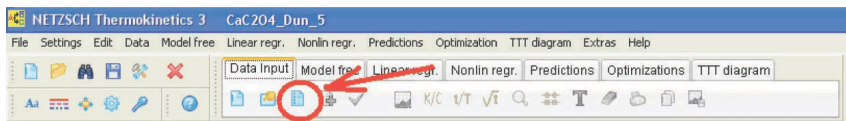


Figure 4.7: Selection of the type of measurement for loading in the NETZSCH Thermokinetics software.

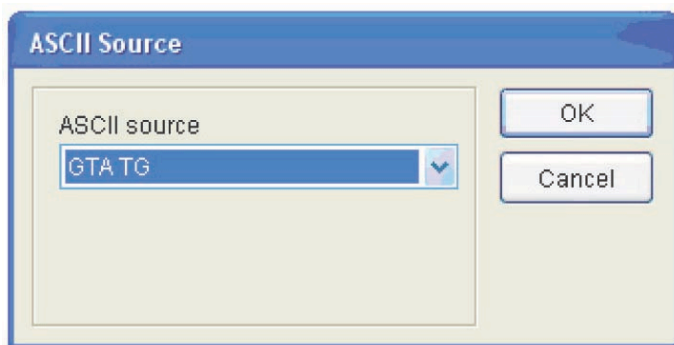


Figure 4.8: Selection of the measurement type for loading in the NETZSCH Thermokinetics software.

The data is loaded by clicking the Load ASCII file icon (Figure 4.9). In the popup window, the user specifies the desired data file.

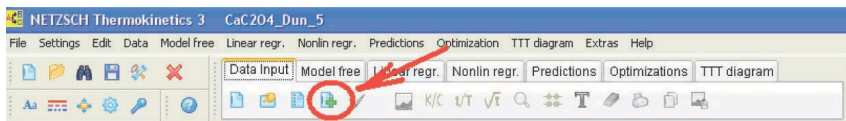


Figure 4.9: Loading data into the NETZSCH Thermokinetics software.

If necessary, the user corrects the evaluation range limits (Figure 4.10).

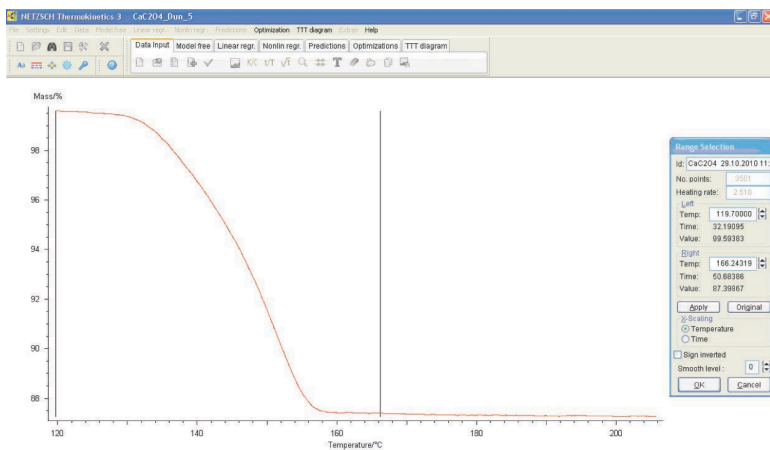


Figure 4.10: Selection of the evaluation range limits in the NETZSCH Thermokinetics software.

The loaded files are checked by clicking the Check scans icon (Figure 4.11).

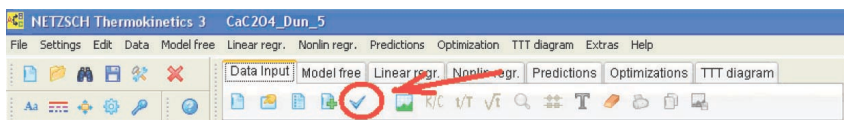


Figure 4.11: Check of the loaded data in the NETZSCH Thermokinetics software.

The next step is to perform the model-free analysis. To do this, the user should enter the Model free menu (Figure 4.12).

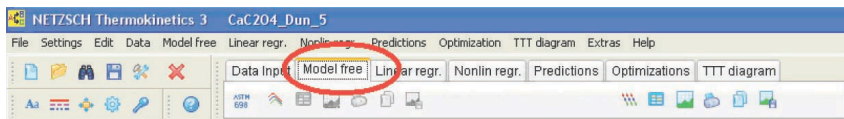


Figure 4.12: Model-free analysis.

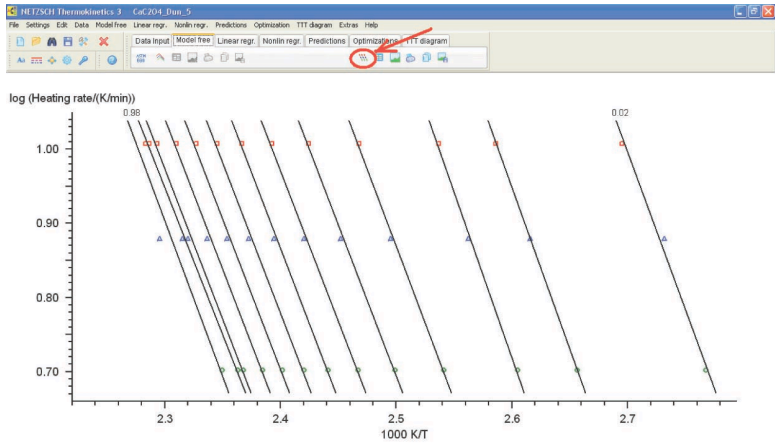


Figure 4.13: Logarithm of heating rate versus inverse temperature.

The Ozawa–Flynn–Wall analysis is started by pressing the corresponding button to show the graph of the logarithm of heating rate versus inverse temperature (Figure 4.13).

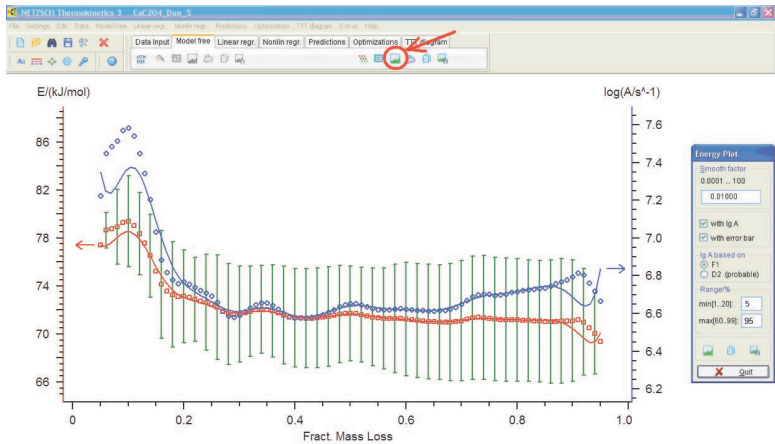


Figure 4.14: Activation energy and preexponential factor versus conversion.

The activation energy and preexponential factor are then calculated as a function of conversion (Figure 4.14). Analogous calculations can be performed by the Friedman method (Figure 4.15).

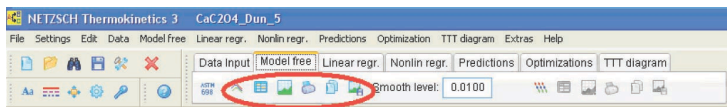


Figure 4.15: Model-free Friedman analysis.

The resulting activation energies and preexponential factors are used as a zero approximation to solve the direct kinetic problem. To do this, the *Linear regr.*-toolbar is used (Figure 4.16). This procedure is applicable to one-step processes.

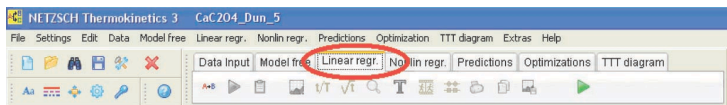


Figure 4.16: Linear regression.

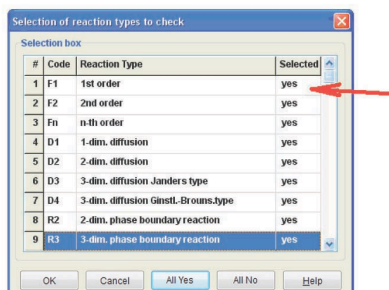
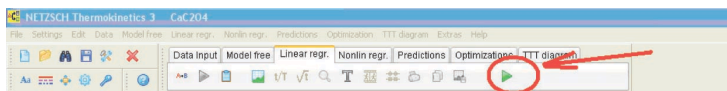


Figure 4.17: Model selection in case of linear regression.

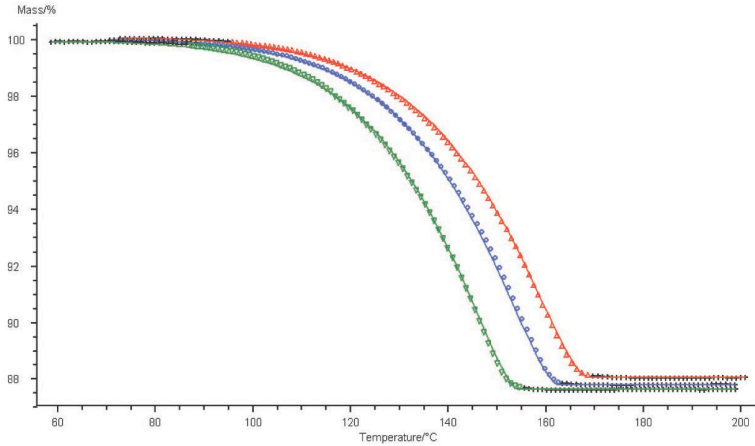


Figure 4.18: Graphical comparison of the computation results (solid line) and experimental data (symbols) for TG curves of the $\text{CaC}_2\text{O}_4 \cdot \text{H}_2\text{O}$ dehydration. Three heating rates; one-step reaction.

Results using Model: s: Bna

Parameters Statistics Termination Criteria Regression Values F-test: Fit Quality F-test: Step Significance

#	Parameter Name	Initial Value	Optimum Value	Sign.	t*S(Par)
0	log A1/s ⁻¹	6.3163	6.5171		4.8863E-2
1	E1 kJ/mol	70.3493	71.0987	+	0.4291
2	Reactord. 1	0.1381	0.3110	+	2.1742E-2
3	Exponent a1	8.3887E-2	5.5752E-2	+	1.2667E-2
4	Mass Loss1/%	-11.9682	-11.9682		constant
5	Mass Loss2/%	-12.1762	-12.1762		constant
6	Mass Loss3/%	-12.2892	-12.2892		constant

Cancel Save Results as Default Print Printer Font

Figure 4.19: Kinetic parameters of the $\text{CaC}_2\text{O}_4 \cdot \text{H}_2\text{O}$ dehydration.

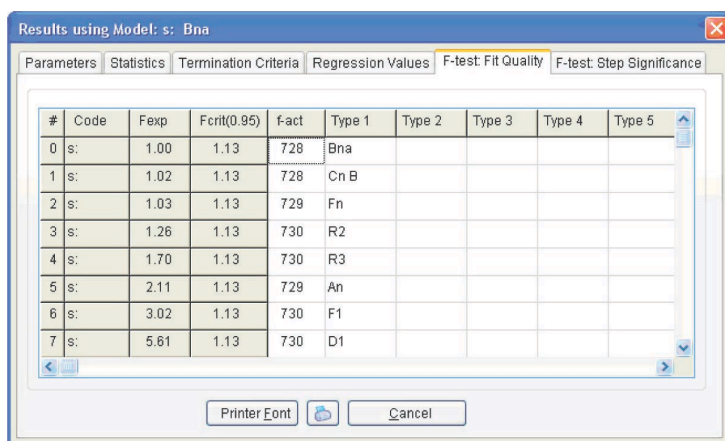
If the kinetic model of a process is a priori unknown, it is advisable to perform calculations using all models (Figure 4.17). To do this, in the Selection box, the

user should click on ‘Yes’ in the corresponding cell of the column ‘Selected’. The program outputs a graph of measured and calculated curves, as well as tables.

4.3 Analysis of Computation Results

Let us consider the computation results obtained by the linear regression method for the $\text{CaC}_2\text{O}_4 \cdot \text{H}_2\text{O}$ dehydration (Figure 4.19).

Figure 4.19 presents the Arrhenius parameters and the form and characteristics of the function best fitting the experimental results (from the statistical view-point). For the reaction under consideration, the best fitting function is the Prout–Tompkins equation with autocatalysis (the Bna code), which is indicated at the top left of the table. However, before discussing the meaning of the results obtained, let us consider the F-test: Fit Quality window (Figure 4.20).



#	Code	Fexp	Fcrit(0.95)	fact	Type 1	Type 2	Type 3	Type 4	Type 5
0	s:	1.00	1.13	728	Bna				
1	s:	1.02	1.13	728	Cn B				
2	s:	1.03	1.13	729	Fn				
3	s:	1.26	1.13	730	R2				
4	s:	1.70	1.13	730	R3				
5	s:	2.11	1.13	729	An				
6	s:	3.02	1.13	730	F1				
7	s:	5.61	1.13	730	D1				

Figure 4.20: Fit quality for different models.

4.3.1 The F-test: Fit quality and F-test

Step significance windows present the statistical analysis of the fit quality for different models. This allows us to determine using the statistical methods which of the models provides the best fit for the experimental data.

To perform such an analysis, Fisher’s exact test is used. In general, Fisher’s test is a variance ratio which makes it possible to verify whether the difference between two independent estimates of the variance of some data samples is significant. To do this, the ratio of these two variances is compared with the corre-

sponding tabulated value of the Fisher distribution for a given number of degrees of freedom and significance level. If the ratio of two variances exceeds the corresponding theoretical Fisher test value, the difference between the variances is significant.

In the Thermokinetics software, Fisher's test is used for comparing the fit qualities ensured by different models. The best-fit model, that is, the model with the minimal sum of squared deviations, is taken as a reference (conventionally denoted as model 1). Then, each model is compared to the reference model. If the Fisher test value does not exceed the critical value, the difference between current model 2 and reference model 1 is insignificant. There is no reason to then believe that model 1 provides a more adequate description of the experiment in comparison to model 2.

The F_{exp} value is estimated by means of Fisher's test:

$$F_{exp} = \frac{LSQ_1/f_1}{LSQ_2/f_2}. \quad (4.2)$$

The F_{exp} value is compared with the Fisher distribution $F_{crit}(0.95)$ for the significance level of 0.95 and the corresponding number of degrees of freedom.

Figure 4.20 shows that three models meet this requirement: the Prout–Tompkins n th-order equation with autocatalysis (Bna), the n th-order equation with autocatalysis (Cnb), and the n th-order reaction (Fn) (see Table 3.1). To discriminate between these functions, a nonlinear regression calculation is performed for each function separately under the assumption of a one-step process. To do this, the Nonlin regr. toolbar is opened (Figure 4.21).

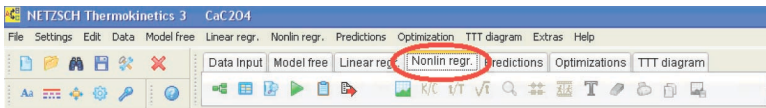


Figure 4.21: Nonlinear regression.

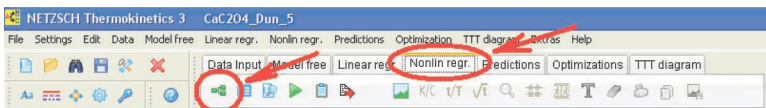


Figure 4.22: Menu for model selection.

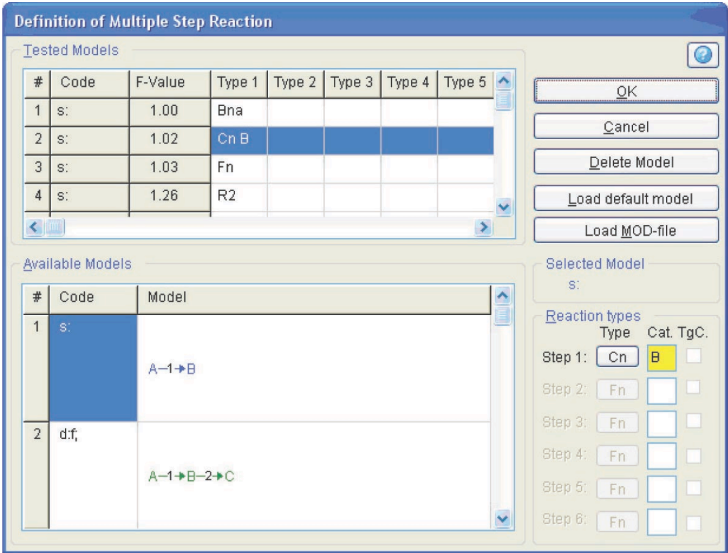


Figure 4.23: Selection of the model and function type in the nonlinear regression menu.

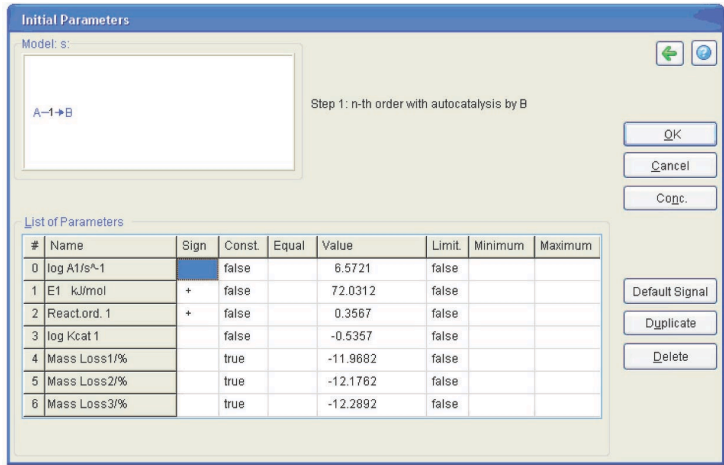


Figure 4.24: Table of initial parameters.

In this toolbar, the Model Selection button is pressed (Figure 4.22) to select the process model. In the opened window (Figure 4.23), we select the one-step process and the Cn model (n th order reaction with autocatalysis). The program is started by clicking on the green triangular button (Figure 4.22). The table of initial parameters that should be verified then appears (Figure 4.24).

In the Const. column, the option 'false' is set for the parameters that should be varied and the option 'true' is chosen for the parameters that remain constant. The three columns to the right of this column are intended for imposing constraints on the selected values. The computation results are presented in Figure 4.25.

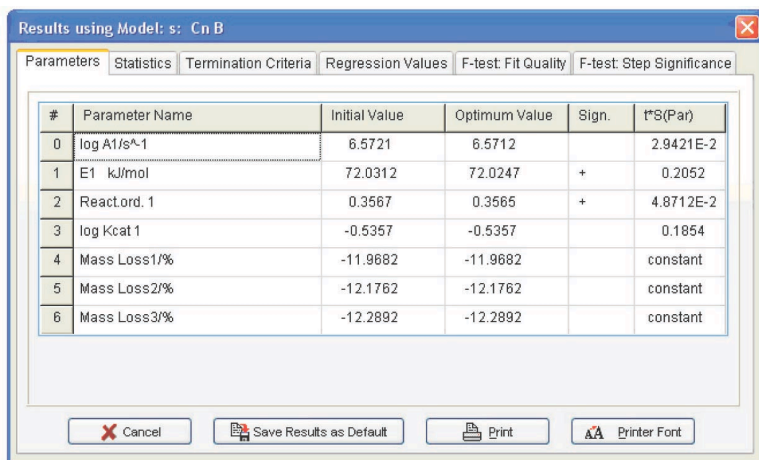


Figure 4.25: Computation results for the Cnb function.

The calculation for the Fn function is performed analogously. The results are shown in Figure 4.26. To compare the parameter values obtained for three statistically equivalent functions, these parameters should be evaluated with allowance for correlation of the initial data. In the Statistics menu (Figure 4.25), the Durbin–Watson test value is presented (4.3) which should be added to the calculated tS error, where t is the Student's test for a given number of degrees of freedom, and S is the mean-square deviation. Thus, we obtain the following set of parameters and their errors (Table 4.1) for all statistically equivalent functions.

#	Parameter Name	Initial Value	Optimum Value	Sign.	t*S(Par)
0	log A1/s ⁻¹	6.7290	6.7290		6.8869E-3
1	E1 kJ/mol	73.1002	73.1002	+	6.4281E-2
2	Reactord. 1	0.2592	0.2592	+	1.2542E-2
3	Mass Loss1/%	-11.9682	-11.9682		constant
4	Mass Loss2/%	-12.1762	-12.1762		constant
5	Mass Loss3/%	-12.2892	-12.2892		constant

Figure 4.26: Computation results for the Fn function.

The following conclusions can be drawn from Table 4.1: first, the autocatalysis parameters for the Bna and CnB functions are almost zero, that is, all is reduced to the Fn function. Second, the error of the Arrhenius parameters for Fn are minimal. Hence, the calcium oxalate dehydration is better described by the n th-order function. The reaction order can be considered to be $1/3$, that is, the process is described by the “contracting sphere equation.” This means that the sample consists of spherical particles of the same size and that the dehydration is a homothetic process, that is, the particles during decomposition undergo a self-similar decrease in size. Such a mechanism is inherent in thermolysis of inorganic crystal hydrates. Thus, the problem of $\text{CaC}_2\text{O}_4 \cdot \text{H}_2\text{O}$ dehydration macrokinetics can be thought of as solved.

Function code	log A	E, kJ/mol	Reaction order n	log K cat 1	Exp a1
Bna	6.8±0.6	73±6	0.34±0.25	—	0.06±0.14
CnB	6.8±1.0	74±8	0.41±0.48	-0.45±1.9	—
Fn	7.0±0.1	75.2±0.8	0.34±0.25	—	—

Table 4.1: Kinetic parameters of the $\text{CaC}_2\text{O}_4 \cdot \text{H}_2\text{O}$ dehydration process

The project created in the NETZSCH Thermokinetics software is saved by clicking on the common button (Figure 4.27).

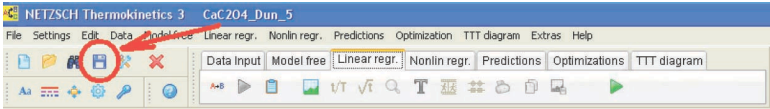


Figure 4.27: Saving the project in the NETZSCH Thermokinetics software.

The output data of the NETZSCH Thermokinetics software can be exported as an ASCII file by clicking on a button in the *Nonlin regr.* toolbar (Figure 4.28). In the opened dialog box, the user can select data that must be exported: kinetic parameters, statistics, and so on. (Figure 4.29).

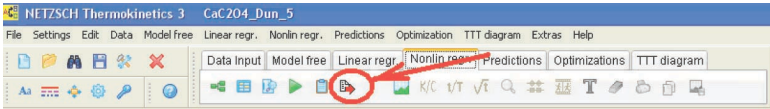


Figure 4.28: Export of the results from NETZSCH Thermokinetics as an ASCII file.

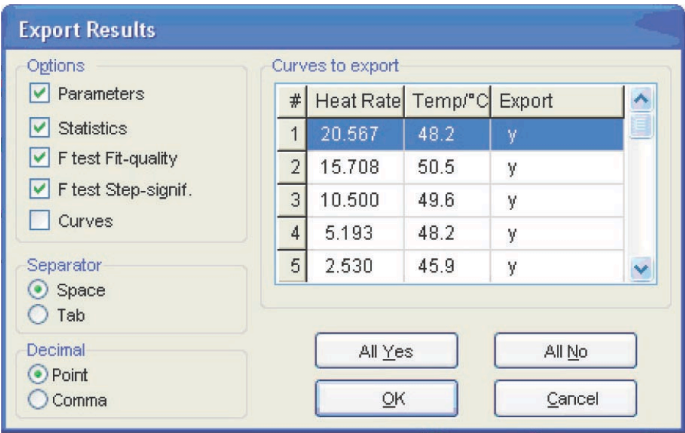


Figure 4.29: Selection of data for export as an ASCII file.

Chapter 5

Kinetic Analysis Based on Differential Scanning Calorimetry Data

The procedure of kinetic analysis of a reaction based on DSC experiment data can be exemplified by the curing of an epoxy resin. The curing reaction involves the opening of the epoxy ring by amine and is accompanied by an exotherm, which is recorded on a differential scanning calorimeter. The fraction of the cured resin is directly proportional to the evolved heat quantity. The knowledge of how the conversion (that is, the fraction of the reacted resin) depends on time and temperature provided by DSC enables one, in studying actual epoxy binders, to optimize the conditions of their treatment and the forming of products, for example, a polymer composite material. It is worth noting that curing occurs without weight change. TG measurements are therefore inapplicable in this case.

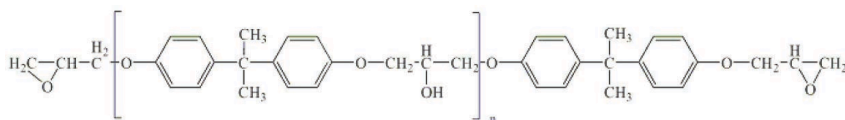


Figure 5.1: Chemical structures of the epoxy diene resin based on bisphenol A.

It is well known [11], that, depending on the composition of reagents and process conditions, curing would occur as a one-stage as well as a two-stage process. In the present section both variants are considered.

Let us consider a classical system consisting of an epoxy diene resin based on 4,4'-dihydroxydiphenylpropane (bisphenol A) (Figure 5.1) and a curing agent, metaphenylenediamine (Figure 5.2). The curing of this system was studied on a Netzsch DSC-204 Phenix analyzer. Measurements were taken at five heating rates: 2.5, 5, 7.5, 10, and 15 K/min. Samples were placed in Netzsch aluminum crucibles with a lid. A hole was preliminarily made in the lid. The process was carried out in an argon flow at a flow rate of 100 mL/min. A mixture of the resin components were freshly prepared before taking measurements. The samples were 5–5.5 mg for each of the heating rates.

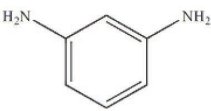


Figure 5.2: Chemical structure of the curing agent, metaphenylenediamine.

5.1 Computation Procedure. Solution of the Inverse and Direct Kinetic Problems. Quasi-One-Stage Process

Experimental data acquired using the NETZSCH equipment is processed with the NETZSCH Proteus program. Figure 5.3 demonstrates that the curing of an epoxy resin in the given temperature range can be considered quasi-one-stage at all heating rates used.

The procedure of kinetic analysis for DSC data is analogous to that for TG measurements described above. Here, we focus on the differences between these procedures. First of all, when loading data in the NETZSCH Thermokinetics software, the user select Differential Scanning Calorimetry as the type of measurement (Figure 5.4).

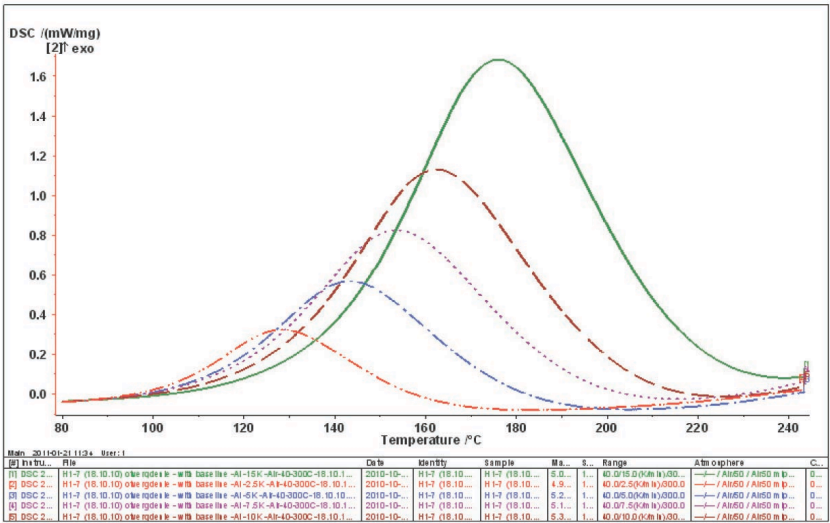


Figure 5.3: DSC curves of the curing of an epoxy resin at five heating rates.

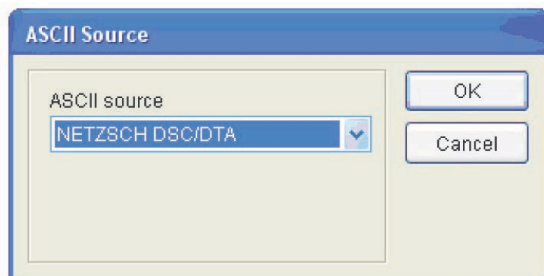


Figure 5.4: Selection of the type of measurement for loading in the NETZSCH Thermokinetics software.

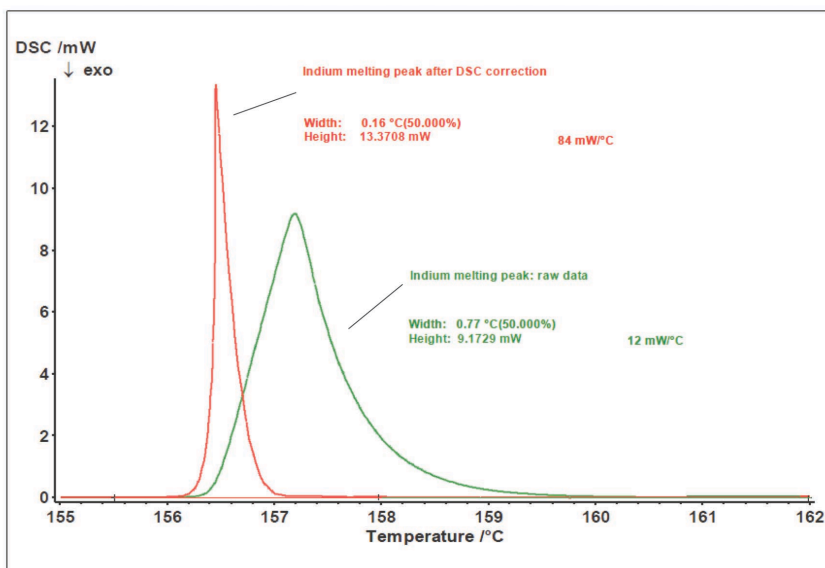


Figure 5.5: Example of the change in the peak shape for indium metal melting after the correction of the DSC signal (reprinted with permission from [9] © NETZSCH-Gerätebau GmbH).

The DSC results not only provide information on the transformation of an analyte, but also depend on the heat exchange conditions in the analyzer-sample

system. Because of the thermal resistance between the sample and the sensor, the thermal flow released as a result of processes in the sample is smeared in time (Figure 5.3). To correctly perform kinetic analysis, the true signal shape should be found, that is, data should be corrected for the time constant of the instrument and for thermal resistance. These corrections can be applied with the DSC Correction routine.

As a rule, the melting peak of pure metal (indium in this case) serves as the calibration measurement for determining the correction parameters. This metal is chosen because it melts in the same temperature range in which the epoxy resin is cured. The path to the file with preliminarily calculated correction parameters is specified in the same window (Figure 5.6).

Project Initialization

Project name: Epoxy

Material: Epoxy

No of Scans[1..16]: 5

Type of measurement: Differential Scanning Calorimetry

Direction of exotherm: Up

Parameters of Diff. contr.: not used

Type of math. weight: w = 1

Correction parameters: Sn_10K.kcr

Tested models:

#	Code	Type 1	Type 2	Type 3	Type 4	Type 5
1						
2						
3						

Remarks:

Buttons: OK, Cancel, Diffusion contr. (checkbox), Change Corr Par, Clear Remarks

Figure 5.6: Project initialization for DSC measurements.

The data is loaded by clicking the Load ASCII file icon (see Figure 4.9), analogously to the procedure with TG data. If necessary, the user corrects the evaluation range limits (Figure 5.7). For further calculation, the type of baseline should be selected (Figure 5.8). In this case, we use a linear baseline.

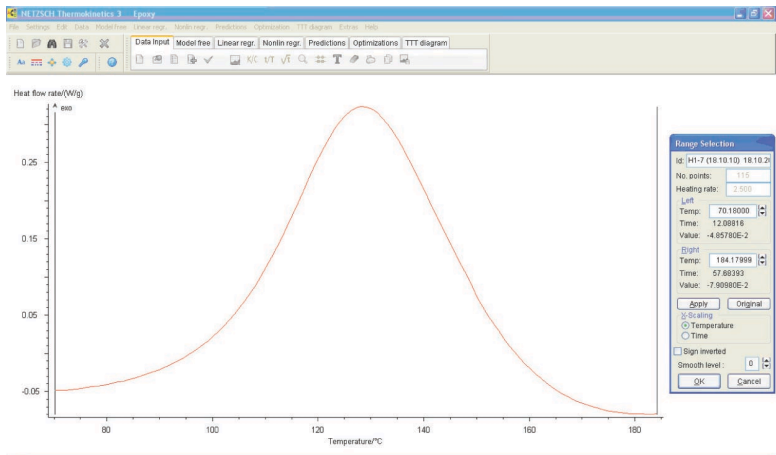


Figure 5.7: Selection of the evaluation range limits in the NETZSCH Thermokinetics software.

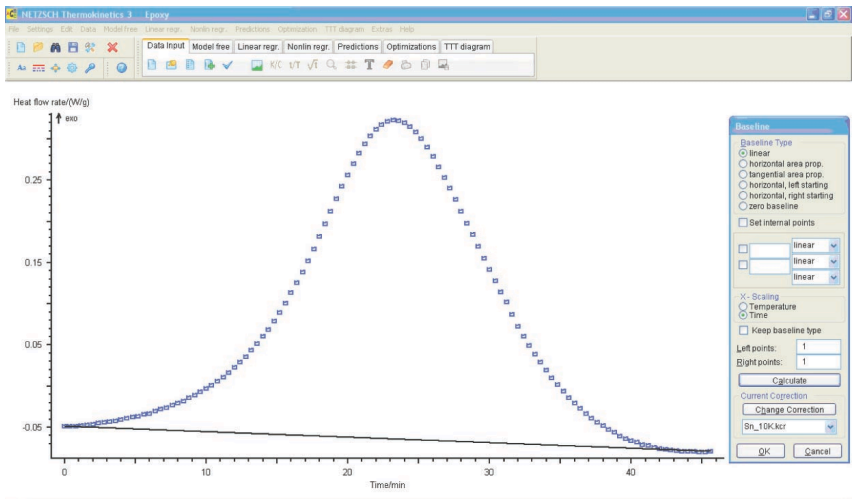


Figure 5.8: Choice of the baseline.

The loaded data is checked and model-free analysis is performed (Figure 5.9).

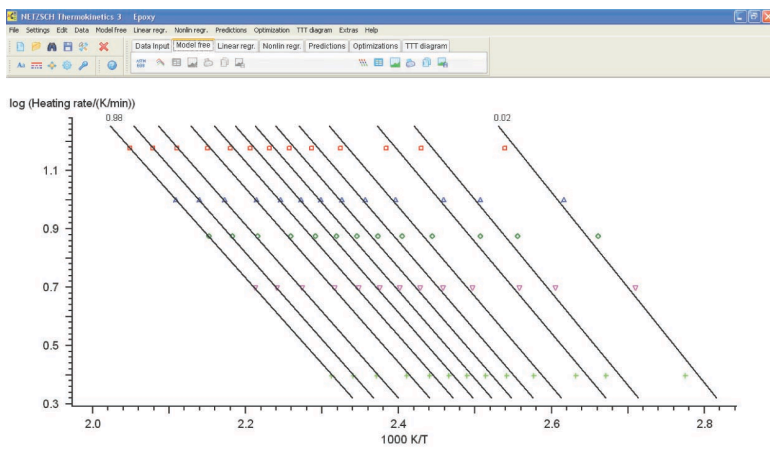


Figure 5.9: Logarithm of heating rate versus inverse temperature (calculation by the Ozawa–Flynn–Wall method).

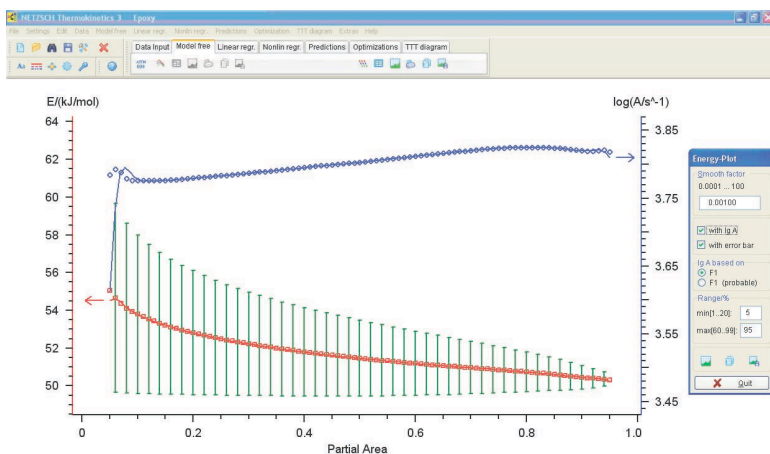


Figure 5.10: Activation energy and preexponential factor versus conversion (calculation by the Ozawa–Flynn–Wall method).

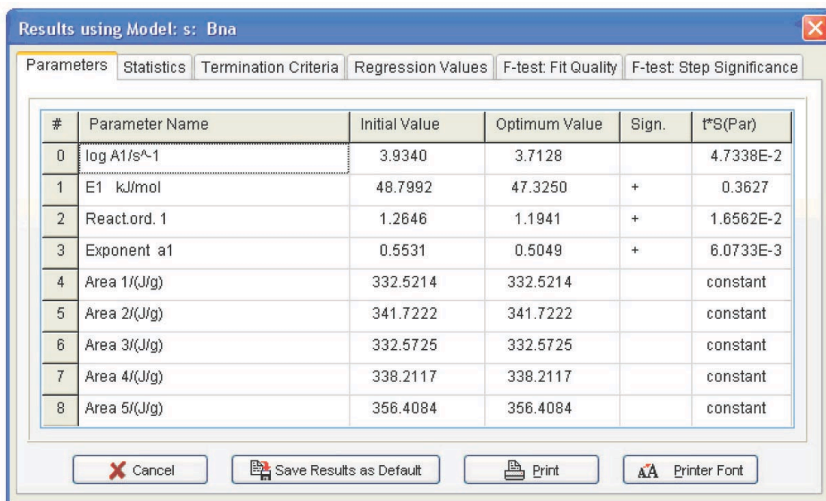
The resulting activation energies and preexponential factors are used as a zero approximation in solving the direct kinetic problem.

5.2 Analysis of Computation Results

Let us consider, first of all, the computation results (Figure 5.11) obtained by the linear regression method under the assumption of a one-stage process.

Figure 5.11 presents the Arrhenius parameters, the form of function, and its characteristics best fitting the experimental results (from the statistical view-point). The calculation was performed for all models. As expected, however, the only relevant model turned out to be the model of reaction with autocatalysis described by the Prout–Tompkins equation (Bna code) (Figure 5.12), which is indicated at the top left of the table showed in Figure 5.11.

Refinement of the model parameters by the nonlinear regression method led to results analogous to those in Figure 5.11. The statistical characteristics of the model are shown in Figure 5.13. With the inclusion of the Durbin–Watson test value, the resulting model parameters are as follows: $E = 47 \pm 3$ kJ/mol, $\log A = 3.7 \pm 0.4$, $n = 1.2 \pm 0.15$, $a1 = 0.50 \pm 0.05$.



#	Parameter Name	Initial Value	Optimum Value	Sign.	t* S(Par)
0	log A1/s ⁻¹	3.9340	3.7128		4.7338E-2
1	E1 kJ/mol	48.7992	47.3250	+	0.3627
2	Reactord. 1	1.2646	1.1941	+	1.6562E-2
3	Exponent a1	0.5531	0.5049	+	6.0733E-3
4	Area 1/(J/g)	332.5214	332.5214		constant
5	Area 2/(J/g)	341.7222	341.7222		constant
6	Area 3/(J/g)	332.5725	332.5725		constant
7	Area 4/(J/g)	338.2117	338.2117		constant
8	Area 5/(J/g)	356.4084	356.4084		constant

Figure 5.11: Arrhenius parameters obtained by non-linear regression.

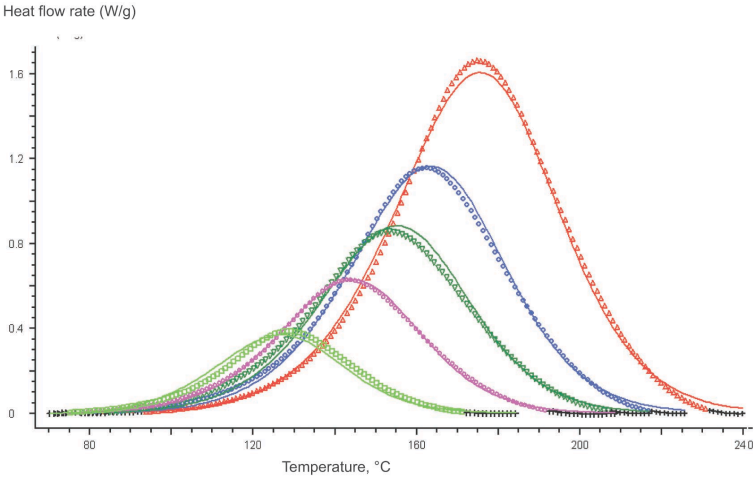


Figure 5.12: Graphical comparison of the computation results (solid line) and experimental data (symbols) for DSC curves of the epoxy resin curing process. Five heating rates; one-step reaction; the Prout–Tompkins equation.

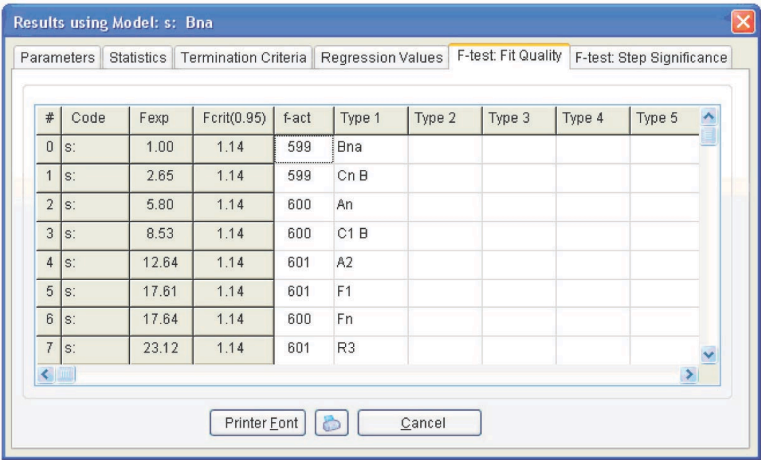


Figure 5.13: Statistical analysis of quality fits for different models.

As is known, the epoxy resin curing reaction occurs due to the autocatalysis mechanism [12]. The reaction is promoted by hydroxyl groups formed upon cross-linking [11]. At the early step of the reaction, the reaction rate increases with an increase in the conversion because of the catalytic effect of the reaction product. With a lapse of time, the amount of the starting reagent decreases, and so does the reaction rate. Thus, the plot of the reaction rate versus time passes through a maximum. In the simplest case, this mechanism is described by the Prout–Tompkins function, which also follows from our preliminary calculation. However, the curing process is known to comprise at least two independent steps. This function is therefore often unable to adequately describe the curing process. It is more preferable to use the following equation for calculation of the curing process [11]:

$$\frac{d\alpha}{dt} = (k_1 + k_2\alpha^m)(1 - \alpha)^n, \text{ where } k_i = A_i e^{\frac{-E_{a_i}}{RT}} \quad (5.1)$$

In the software, this equation is represented as a model with two parallel reactions: a reaction with autocatalysis described by the Prout–Tompkins equation (Bna) and an n th order equation (Fn).

Results using Model: d;p: Bna Fn

#	Parameter Name	Optimum Value	Sign.	t*S(Par)
0	log A1/s ⁻¹	3.7503		9.8585E-2
1	E1 kJ/mol	47.3124	+	0.8004
2	Reactord. 1	1.3226	+,lim	3.2641E-2
3	Exponent a1	0.6233	+	3.0456E-2
4	log A2/s ⁻¹	2.3943		0.5145
5	E2 kJ/mol	48.1048	+	3.7067
6	Reactord. 2	0.3746	+,lim	8.6708E-2
7	Area 1/(J/g)	332.5214		constant
8	Area 2/(J/g)	341.7222		constant

Cancel Save Results as Default Print Printer Font

Figure 5.14: Kinetic parameters for the two-step model.

Model with two parallel reactions: a reaction with autocatalysis described by the Prout–Tompkins equation and an n th order reaction (Fn). The kinetic param-

eters corresponding to a two-step model with two parallel reactions are presented in Figure 5.14. However, the difference between the fits provided by the one- and two-stage models is statistically insignificant, as follows from Figure 5.15. In both cases, the F_{exp} value does not exceed the critical value. We may assume that the one- and two-step processes are equiprobable. This phenomenon can be explained by the presence of hydroxyl groups in the initial resin: even at a zero conversion rate, catalytic sites exist, and the autocatalytic mechanism prevails during the entire course of the reaction.

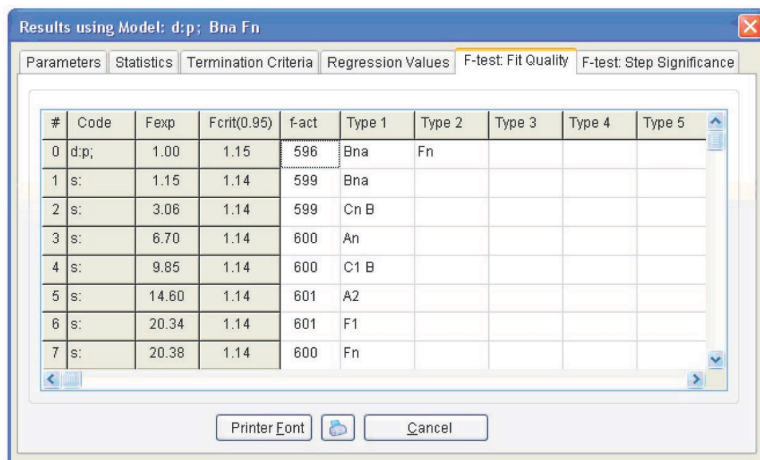


Figure 5.15: Statistical analysis of the fit quality for different models.

Table 5.1 presents the calculation results for both models. As is seen, the errors of the Fn function parameters for the two-stage process are significant, whereas the average parameter values do not differ from those of the Bna function. Hence, we can state that the above calculation does not confirm the occurrence of the two-stage curing process.

Function code	$\log A$	E , kJ/mol	Reaction order n	Exp $a1$
Bna	7.7 ± 0.4	47 ± 3	1.2 ± 0.15	0.50 ± 0.05
Bna	3.75 ± 0.7	47 ± 6	1.3 ± 0.2	0.6 ± 0.2
Fn	2.4 ± 5.0	48 ± 26	0.4 ± 0.6	—

Table 5.1: Parameters for the one- and two-stage models.

5.3 Plotting the Conversion-Time Curves

The above calculation can be successfully used for selecting optimal conditions for the curing process (temperature and time). Let us consider how to obtain the conversion versus time plot (at a given temperature) from the calculated data. To do this, we open the Predictions toolbar. The curves are shown in Figure 5.16. In this case, calculations are performed assuming the kinetic control of the reaction. In reality, once a certain curing degree has been achieved, the initially liquid sample is converted to the viscous flow and then to the solid state. The diffusion of resin and curing agent molecules thereby slows down, and the process becomes diffusion-controlled. Thus, the kinetic calculation should be completed with measurements of the rheological properties of the system. The resulting relationships show that the resin is completely cured within 16 min at 153 °C.

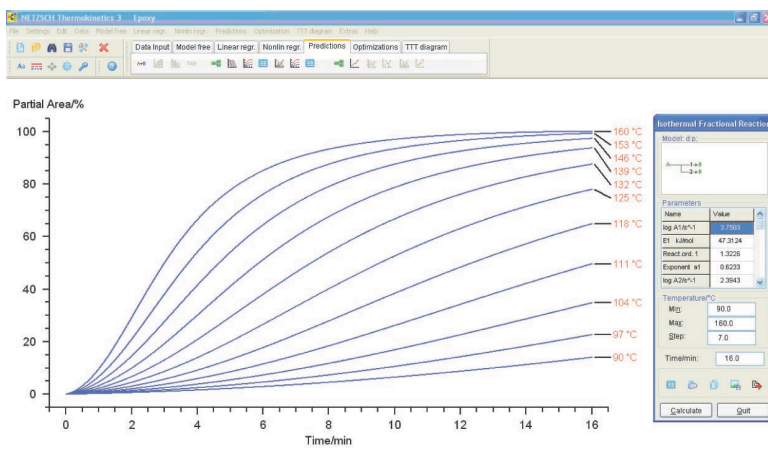


Figure 5.16: Degree of curing of the resin versus the time of exposure of the sample to constant temperature.

Chapter 6

Analysis of Multistage Processes

For multistage process, it is recommended to perform kinetic analysis using the following algorithm. Kinetic analysis is performed separately for each of the stages of the process as for a one-stage reaction, and the corresponding kinetic model and kinetic parameters are determined. Then, kinetic analysis is performed for the entire process using the data obtained for the model of each stage. In so doing, the kinetic parameters of each stage are refined. Thus, when the process is studied as a whole, there is already no need to try different kinetic models since they have been chosen for each stage.

However, for most multistage processes, the effects overlap. To separate quasi-one-stage processes, the Peak Separation software can be used. In general case reaction steps are dependent, so the separation procedure is formal. Obtained peaks does not refer to the single reactions and may be used just for the initial approximation of the Arrhenius parameters. In the case of the independent reactions separated peaks refer to the single reactions and thus may be used for calculation of the Arrhenius parameters.

6.1 Peak Separation Software

In multistage processes with competing or parallel reactions, separate stages, as a rule, overlap, which can lead to considerable errors in the calculated Arrhenius parameters and to an incorrect choice of the scheme of the processes. This in turn will lead to significant errors of the nonlinear regression method because of the nonlinearity of the problem. To solve this problem, the experimental curve is represented by a superposition of separate one-stage processes. This procedure is implemented in the NETZSCH Peak Separation software (Figure 6.1).

The NETZSCH Peak Separation software [13] fits experimental data by a superposition of separate peaks, each of which can be described by one of the following functions:

1. Gaussian function,
2. Cauchy function,

3. pseudo-Voigt function (the sum of the Gaussian and Cauchy functions with corresponding weights),
4. Fraser–Suzuki function (the asymmetric Gaussian function),
5. Pearson function (monotonic transformation from the Gaussian to the Cauchy function),
6. modified Laplace function.

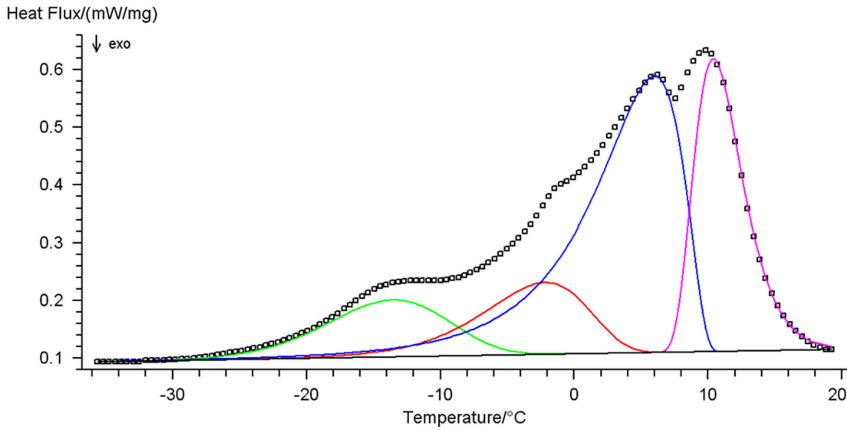


Figure 6.1: Peak separation using the Peak Separation software (reprinted with permission from [13] © NETZSCH-Gerätebau GmbH).

In thermal analysis, chemical reaction steps are described in most cases by the Fraser–Suzuki function (asymmetric Gaussian function). For other processes, e.g., polymer melting, the modified Laplace function must be used. Figure 6.1 shows the decomposition of a multimodal curve with the use of this function and its analytical representation. The Fraser–Suzuki function (asymmetric Gaussian function) and its graphical representation are given below.

$$y_{Fraser} = Ampl \cdot \exp \left[-\ln 2 \left(\frac{\ln [1 + 2 \cdot Asym \cdot (x - Pos)/Hwd]}{Asym} \right)^2 \right] \quad (6.1)$$

$$A_{Fraser} = 0.5 \cdot \sqrt{\pi/\ln 2} \cdot Ampl \cdot \exp \left[\frac{Asym^2}{4\ln 2} \right]. \quad (6.2)$$

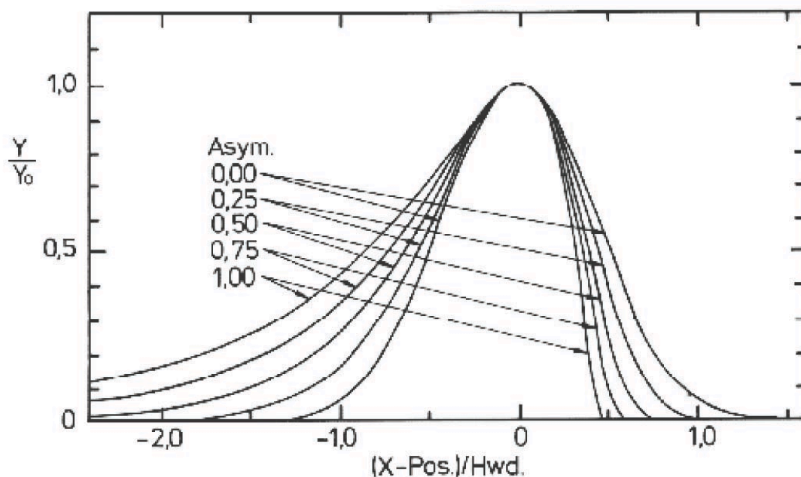


Figure 6.2: Graph of the Fraser–Suzuki function (reprinted with permission from [13] © NETZSCH-Gerätebau GmbH).

The software outputs the following parameters:

1. the optimal curve parameters and their standard deviations,
2. statistical parameters characterizing the fit quality (correlation coefficient and so on.),
3. the initial and simulated curves with the graphs of separate peaks,
4. calculated areas under separate peaks and their contribution to the total area under the curve.

6.2 Multiple Step Reaction Analysis as Exemplified by the Carbonization of Oxidized PAN Fiber

First, multimodal curves are decomposed into separate components and parameters of each process are found by the above procedures, assuming that all processes are quasi-one-stage reactions. Then, the phenomenon is described as a whole. For multiple step processes, the program suggests a list of some schemes of similar transformations, and appropriate schemes are selected from this list. The schemes are presented in Figure 1 of the Appendix. The choice of the corresponding scheme is based on some a priori ideas about the character of stages of the process under consideration.

As an example of the kinetic analysis of multistage processes, let us consider the carbonization of oxidized polyacrylonitrile fiber yielding carbon fiber. The results of thermogravimetric analysis are convenient to use as input data (Figure 6.3).

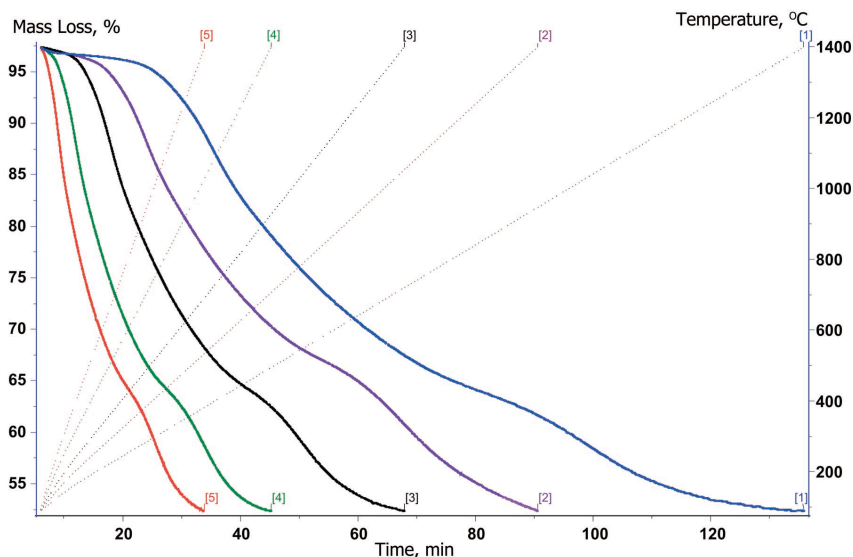


Figure 6.3: Initial TG weight loss curves recorded at different heating rates: (1) 10, (2) 15, (3) 20, (4) 30, and (5) 40 K/min.

The carbonization is a complex process and occurs in several stages [14, 15], which is clearly reflected by the presence of several DTG peaks (Figure 6.4). Kinetic description of a multistage process starts with the decomposition of the complex DTG profile into separate components. It is assumed that the carbonization is, at least, a four-stage process [14, 15]. To separate different stages, the initial DTG curves should be loaded into the Peak Separation software, which provides the best-fit description of the initial process by varying the position, asymmetry, and width of discrete peaks (Figure 6.5) at each heating rate.

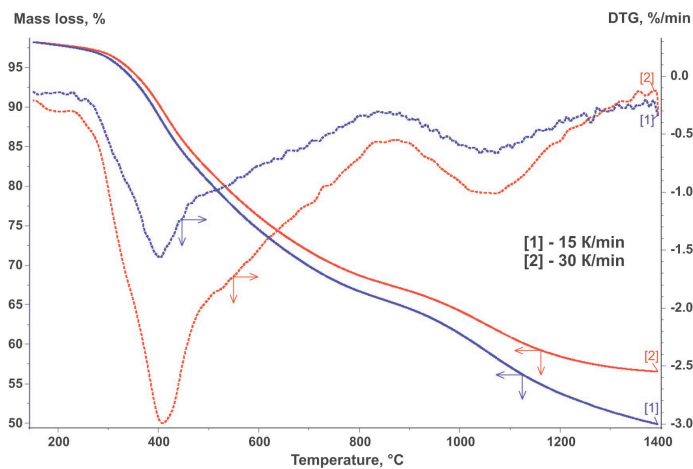


Figure 6.4: DTG curves obtained by differentiation of the initial TG curves recorded at (1) 15 and (2) 30 K/min.

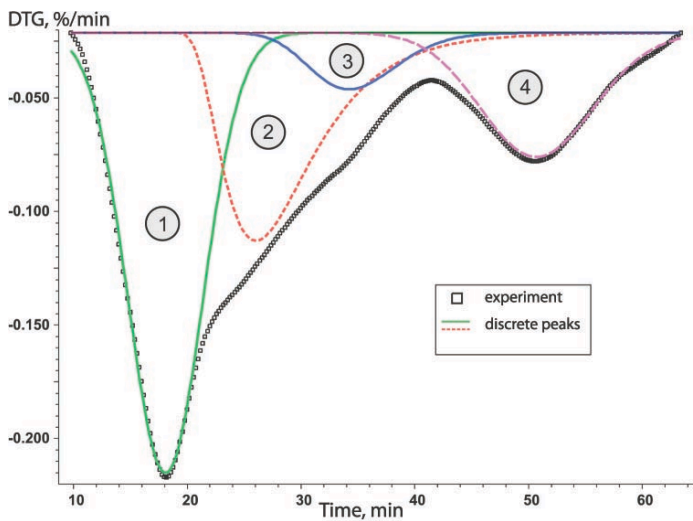


Figure 6.5: Decomposition of the overall DTG profile (10 K/min) into components with the Peak Separation software.

Then, the resulting peaks are sorted on the basis of the number of stage and the inverse kinetic problem is solved. As a result, we obtain the type of model for the given stage and approximate Arrhenius parameters. As a rule, several models of comparable statistical significance satisfy the solution of this problem. If no information is available on the true mechanism of the process, both variants are used for solving the direct kinetic problem.

The estimated parameters and types of models calculated at this step of calculations are listed in Table 6.1, and statistical data of the calculation is presented in Table 6.3. In Table 6.1, the “apparent” activation energy is expressed in kelvins since the notion of mole has no physical meaning for fiber. The E_a/R constant is the temperature coefficient of the reaction rate.

N	Kinetic model	$E_a/R \cdot 10^3 \text{ K}$	$t \cdot S$	$\log A$	$t \cdot S$	n	$t \cdot S$
1	Avrami–Erofeev equation	25.0	0.6	14.8	0.4	0.28	0.3×10^{-3}
2	n th order equation	17.2	0.8	7.2	6.5	3.0	0.13
3	Avrami–Erofeev equation	41.1	2.3	16.2	1.0	0.29	0.1×10^{-3}
4	Avrami–Erofeev equation	54.8	1.3	16.0	0.4	0.32	3.3×10^{-3}

Table 6.1: Estimated kinetic models and parameters of separate stages of the carbonization process.

N	Kinetic model	$E_a/R \cdot 10^3 \text{ K}$	$t \cdot S$	$\log A$	$t \cdot S$	n	$t \cdot S$
1	Avrami–Erofeev equation	26.1	0.6	15.7	0.4	0.25	$4.2 \cdot 10^{-3}$
2	n th order equation	35.5	2.1	18.8	1.2	1.98	0.14
3	Avrami–Erofeev equation	38.3	2.1	16.7	1.0	0.28	$0.1 \cdot 10^{-3}$
4	Avrami–Erofeev equation	56.8	4.7	16.8	1.6	0.19	$0.1 \cdot 10^{-3}$

Table 6.2: Calculated kinetic models and parameters of separate stages of the carbonization process.

Parameter	Stage 1	Stage 2	Stage 3	Stage 4
Least-squares value	22.3	32.0	2.6	7.1
Correlation coefficient	0.9988	0.9926	0.9956	0.9979
Average difference	2.2×10^{-3}	21.0×10^{-3}	8.6×10^{-3}	14.5×10^{-3}
Durbin–Watson test value	2.8×10^{-3}	1.4×10^{-3}	1.6×10^{-3}	1.4×10^{-3}
Durbin–Watson ratio	19.0	26.9	25.0	27.0

Table 6.3: Statistical data of the calculation.

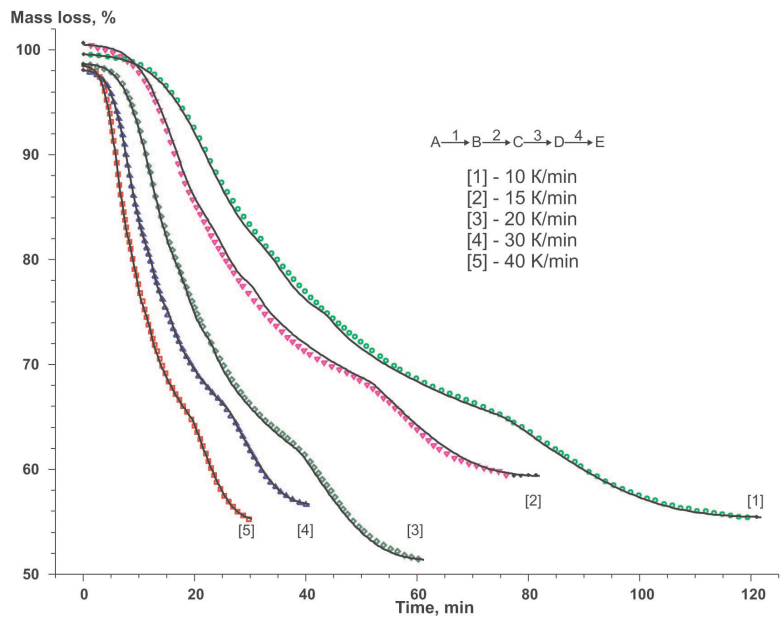


Figure 6.6: Complete kinetic description of experimental data with the use of the model of four successive reactions.

One of the basic tasks of formal kinetic description is to determine the sequence of stages. First, the direct kinetic problem is solved using multivariate nonlinear regression for the successive processes (the qfff scheme in Figure 2 of Appendix, four-stage). Then, for each of the stages, kinetic parameters are refined separately on the basis of statistical tests. As shown by preliminary calculations, stages 1, 3, and 4 are well fitted by the Avrami–Erofeev equation (Equation 3.5) and stage 2, by the n th order equation.

$$f(\alpha) = (1 - \alpha) \cdot n \cdot (-\ln(1 - \alpha))^{\frac{n-1}{n}} \quad (6.3)$$

The calculated results and experimental data for successive processes are compared in Figure 6.6. The kinetic parameters and statistical characteristics of this sequence of stages are presented in Tables 6.4 and 6.5.

Parameter	Value
Least-squares value	1448.7
Correlation coefficient	0.9998
Average difference	0.21
Durbin–Watson test value	5.09×10^{-3}
Durbin–Watson ratio	14.4

Table 6.4: Statistical data of the calculation.

N	Kinetic model	$E_a R$	t•S	log A	t•S	n	t•S
1	Avrami–Erofeev equation	24	3	11	1.5	0.23	1.2×10^{-2}
2	n th order equation	34	7	10	3	5	1
3	Avrami–Erofeev equation	63	5	25	5	0.02	0.1
4	Avrami–Erofeev equation	99	230	53	116	0.8	10

Table 6.5: Calculated kinetic models and parameters of separate stages of the carbonization process for the successive-parallel scheme.

According to the authors [14] carbonization process may be represented by a set of successive-parallel processes. Let us consider this situation (the qfff

scheme in Figure 3 of the Appendix). The results shown in Figure 6.3 and summarized in Table 6.5 have been obtained with the use of the same set of functions.

The F test value for the latter scheme with respect to the former one is $F_{\text{exp}} = 58.6$, $F_{\text{theor}} = 1.11$.

Comparison of the calculation results for each scheme reliably shows that, from the formal kinetic viewpoint, the scheme of successive stages best describes thermoanalytical data as a whole.

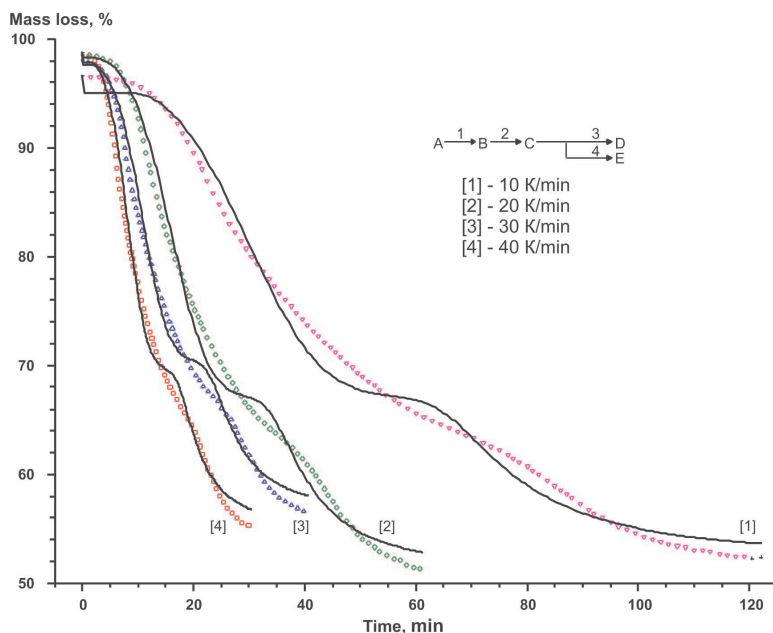


Figure 6.7: Comparison of calculated and experimental data for the scheme of successive-parallel stages.

Thus, formal kinetic analysis makes it possible to choose the type of function best fitting the experimental curves (TG, DTG, DSC), evaluate kinetic parameters, determine the number of stages and their sequence (successive, parallel, etc.). In addition, the statistically optimal kinetic parameters allow one to model temperature change conditions resulting in constant weight loss or enthalpy change rate and obtain dependences of these characteristics under isothermal conditions or in other temperature programs.

Bibliography

- [1] J. Sestak. *Thermophysical Properties of Solids*. Prague: Academia, 1984.
- [2] S. Vyazovkin et al. ICTAC Kinetics Committee Recommendations for Performing Kinetic Computations on Thermal Analysis Data. *Thermochimica Acta* 1 (2011):520.
- [3] V.A. Sipachev and I.V. Arkhangel'skii. Calculation Techniques Solving Non-Isothermal Kinetic Problems. *Journal of Thermal Analysis* 38 (1992): 1283–1291.
- [4] B. Delmon. *Introduction to Heterogeneous Kinetics*. Paris: Technip, 1969.
- [5] P. Barret. *Kinetics in Heterogeneous Chemical Systems*. Elsevier, 1974.
- [6] H.L. Friedman. A Quick, Direct Method for the Determination of Activation Energy from Thermogravimetric Data. *J. Polym. Lett.* 4(5) (1966): 323–328.
- [7] T. Ozawa. A New Method of Analyzing Thermogravimetric Data. *Bull. Chem. Soc. Jpn.* 38 (1965):1881–1886.
- [8] J.H. Flynn and L.A. Wall. A Quick, Direct Method for the Determination of Activation Energy from Thermogravimetric Data. *J. Polym. Sci. Polym. Lett.* 4 (1966):323–328.
- [9] *NETZSCH-Thermokinetics 3.1 Software Help*.
- [10] J. Opfermann. Kinetic Analysis Using Multivariate Non-Linear Regression. *Journal of Thermal Analysis & Calorimetry* 60 (2000):641–658.
- [11] S.Z.D. Cheng. *Handbook of Thermal Analysis and Calorimetry. Applications to Polymers and Plastics*. 3. Elsevier, 2001.
- [12] L. Shechter, J. Wynstra, and R.P. Kurkky. Glycidyl Ether Reactions with Amines. *Ind. Eng. Chem.* 48 (1956):94–97.
- [13] *NETZSCH-Peakseparation 3.0 Software Help*.
- [14] P. Morgan. *Carbon Fibers and Their Composites*. New York: Taylor and Francis, 2005.
- [15] V.Y. Varshavskii. *Carbon Fibers*. Moscow: Varshavskii, 2005.

Appendix

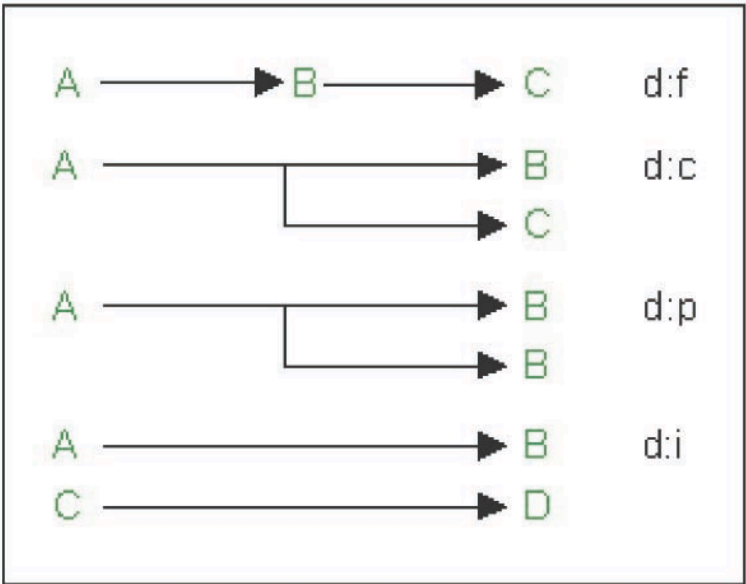


Figure 1: Two-step

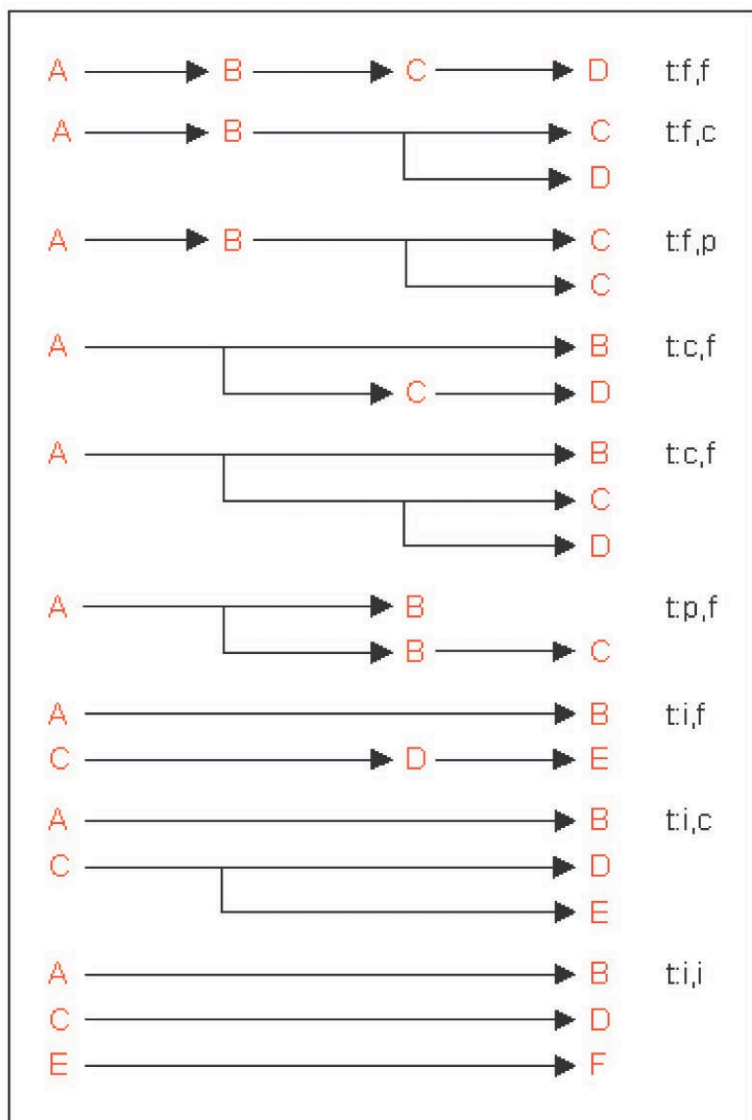


Figure 2: Three-step

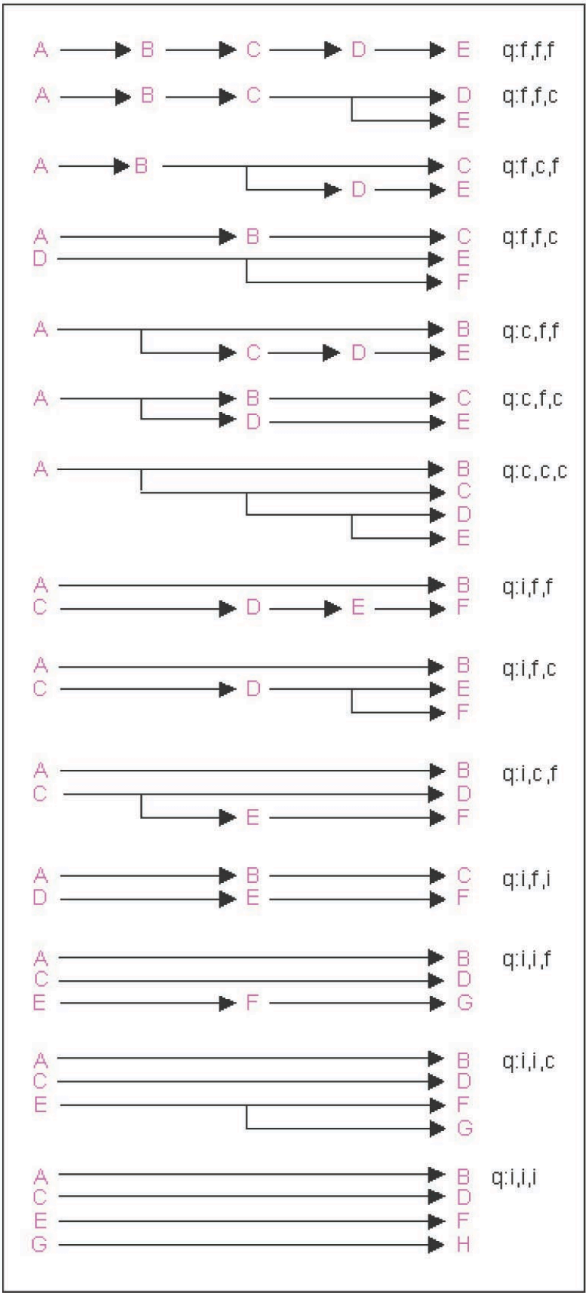


Figure 3: Four-step